Design and Synthesis of Pironetin Analogue/Colchicine Hybrids and Study of Their Cytotoxic Activity and Mechanisms of Interaction with Tubulin ConcepciOn

9 AUTHORS, INCLUDING:

Concepción Vilanova
Universitat Jaume I
8 PUBLICATIONS   7 CITATIONS

Santi Diaz
Universitat Jaume I
48 PUBLICATIONS   241 CITATIONS

Eva Falomir
Universitat Jaume I
86 PUBLICATIONS   1,012 CITATIONS

Isabel Barasoain
Spanish National Research Council
103 PUBLICATIONS   1,603 CITATIONS

Design and Synthesis of Pironetin Analogue/Colchicine Hybrids and Study of Their Cytotoxic Activity and Mechanisms of Interaction with Tubulin

Concepción Vilanova,[†] Santiago Díaz-Oltra,[†] Juan Murga,[†] Eva Falomir,[†] Miguel Carda,[†] Mariano Redondo-Horcajo,[‡] J. Fernando Díaz,*[‡] Isabel Barasoain,*[‡] and J. Alberto Marco*[§]

[†]Departament de Química Inorgànica i Orgànica, Universitat Jaume I, E-12071 Castellón de la Plana, Castellón, Spain
[‡]CIB, Consejo Superior de Investigaciones Científicas, E-28040 Madrid, Spain
[§]Departamento de Química Orgánica, Universitat de València, E-46100 Burjassot, València, Spain

Ⓢ *Supporting Information*

ABSTRACT: We here report the synthesis of a series of 12 hybrid molecules composed of a colchicine moiety and a pironetin analogue fragment. The two fragments are connected through an ester–amide spacer of variable length. The cytotoxic activities of these compounds and their interactions with tubulin have been investigated. Relations between the structure and activity are discussed. Since the spacer is not long enough to permit a simultaneous binding of the hybrid molecules to the colchicine and pironetin sites on tubulin, a further feature investigated was whether these molecules would interact with the latter

through the pironetin end (irreversible covalent binding) or through the colchicine end (reversible noncovalent binding). It has been found that binding to tubulin may take place preferentially at either of these ends depending on the length of the connecting spacer.
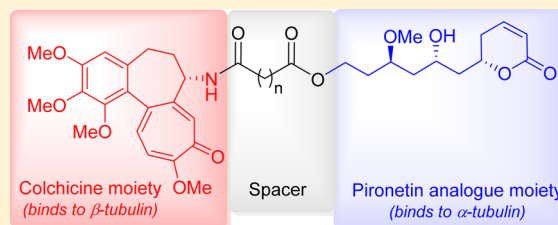
■ INTRODUCTION

Cancer, one major health problem in developed countries,[1] may be induced by many different external and internal causes, including those of the genetic type. Accordingly, various types of pharmacological approaches have been explored.[2,3] One involves the use of cytotoxic drugs, which exert their effect through induction of different methods of cell death.[4] Many such drugs owe this property to interaction with the microtubule network. Microtubules are mainly composed of $\alpha\beta$-tubulin, a heterodimer formed through noncovalent binding of its two monomeric constituents. For normal cell function, microtubules must be dynamic following a process named microtubule dynamic instability.[5] Any molecules which modulate microtubule dynamics will disrupt the dynamics, activating checkpoints that block the cell division process, not only of normal cells but also of tumoral ones. Tubulin-binding molecules (TBMs) are therefore a class of promising molecules to design anticancer agents.

TBMs can be classified depending on the location of their binding site on either α-tubulin or β-tubulin. Compounds that bind to β-tubulin are by far more numerous, their effect being either disruption or stabilization of microtubules. It is interesting to note that archetypal members of this group may behave quite differently: whereas colchicine[6] and the *Vinca* alkaloids such as vinblastine[7] (Figure 1) exert their effects by inducing disruption of microtubules, paclitaxel causes their stabilization (and was the first-described tubulin-binding drug found to do so).[8] Although their effects are in complete

contrast to one another, all these drugs bind to β-tubulin, albeit to different sites within this protein subunit.[5,9,10]

Very few products are known to bind to α-tubulin. The first-reported compound to do so was the naturally occurring 5,6-dihydro-α-pyrone (pironetin).[11] It was subsequently discovered that the peptide-like hemiasterlin family[12] (Figure 2) behaves in the same way. Pironetin, a very potent inhibitor of tubulin assembly, was found to arrest cell cycle progression in the G2/M phase.[13]

Several groups have previously reported structure–activity relationship (SAR) studies on pironetin. The presence of the conjugated C2–C3 double bond and of the oxygen atom at C-9 has been shown to be essential for the biological activity. The presence of a (7R)-hydroxyl group might also be of importance. It has been suggested that a nucleophilic residue, yet to be conclusively identified, of the α-tubulin chain adds in a Michael fashion to the conjugated double bond of pironetin, therefore forming a covalent bond with C-3 of the dihydropyrone ring.[14]

As a final remark, the development of new compounds useful for cancer treatment constitutes a continuous need, due to the emergence of resistances[15] to this therapy, the same phenomenon previously observed with antibiotics.[16]
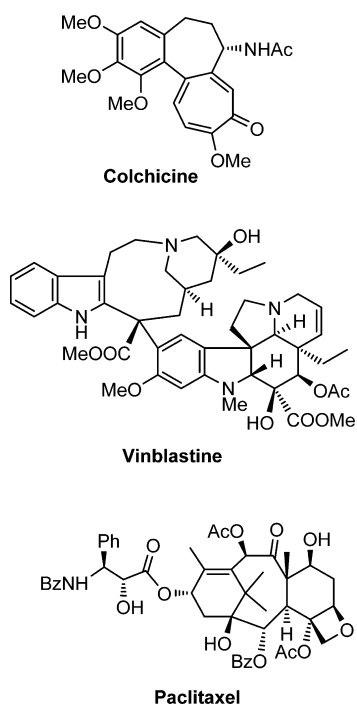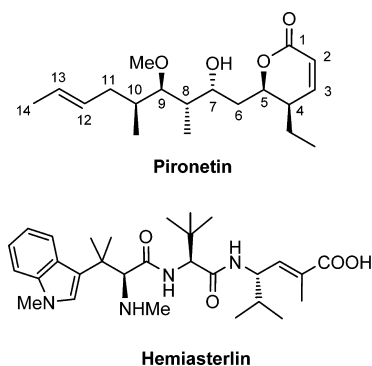
Figure 1. Structures of some natural products reported to selectively bind to β-tubulin.

Figure 2. Structure of two natural products reported to selectively bind to α-tubulin.

◼ CONCEPT AND DESIGN OF HYBRID TUBULIN-BINDING LIGANDS

Pironetin is one of the few members of the group of TBMs that interacts with α-tubulin; thus, it is an interesting target from the pharmacological point of view. The total synthesis of this natural compound has been reported several times in the literature.[17] To develop SAR studies, we started three years ago[18] the design of simplified analogues where all elements that had not yet proven to be essential for the biological activity were removed. The initial target structures **I** and **II** are schematically shown in Figure 3.[18a] On one hand, the conjugated dihydropyrone ring and the side chain with the methoxy group at C-9 were maintained. Furthermore, the hydroxyl group at C-7 was removed in some substrates (**I**) and retained in others (**II**) to see its influence on the activity. On the other hand, not only was the isolated C12−C13 double bond removed, so too were all the alkyl pendants (methyl groups at C-8 and C-10, ethyl at C-4). We then systematically varied the configurations of the two/three remaining stereo-
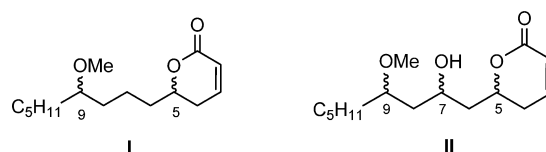

Figure 3. General structures of simplified pironetin analogues of the first generation.[18a]

centers. Proceeding in this way, we prepared all four possible stereoisomers with general constitution **I**, with no hydroxyl group at C-7. Furthermore, we synthesized all eight stereo-isomers exhibiting general structure **II** with a hydroxyl group at C-7.

The cytotoxicity of these analogues and their binding to α/β-tubulin were then studied. Analogues **I** and **II** were found cytotoxic in the low micromolar range, about 3 orders of magnitude less active than the parent molecule. As the latter, they also lead to disruption of the microtubule network.[18a] Moreover, no outstanding differences in cytotoxicity were observed within stereoisomeric compounds of general structure **I** or **II**, the configurations of the stereocenters thus apparently playing a secondary role. Furthermore, we also found that (i) their behavior in cell cultures resembles that of pironetin, (ii) they display a biological mechanism of action very similar to that of this natural compound, and (iii) they compete for the same binding site in α-tubulin.

As an extension of the project, we decided to synthesize cytotoxic TBMs with a potential ability to bind to either α- or β-tubulin and produce a microtubule-destabilizing effect.[19] Since this property is characteristic of both pironetin (binds to α-tubulin) and colchicine (binds to β-tubulin), we decided to prepare tubulin ligands with a hybrid structure[20] such as **1−12** (Figure 4). These molecules display a moiety of colchicine[21] and another of the simplified pironetin type (**21**, *ent*-**21**, and **22**; see Schemes 1 and 2), connected in turn by a spacer of
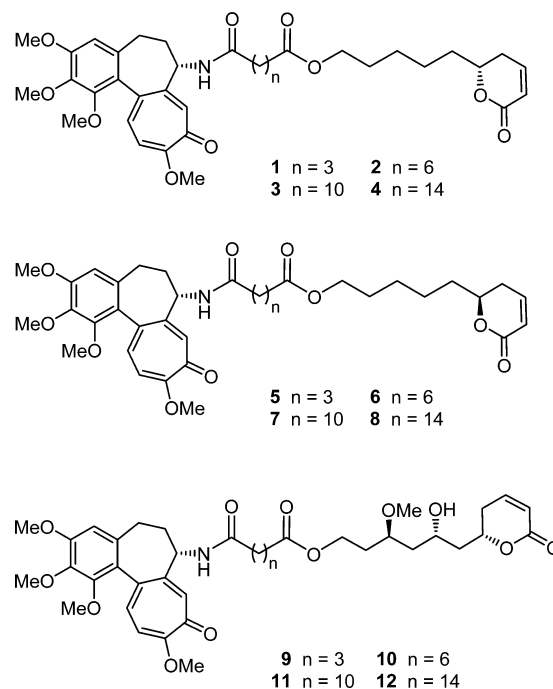

Figure 4. Structures of the pironetin analogue/colchicine hybrids **1**−**12** investigated in this study.

variable length. The stereocenters of the pironetin moiety in compounds 9−12 display the same configurations as in natural pironetin. Although the two respective binding sites in tubulin are too far away for these compounds to act as dual ligands,[22] this strategy should allow us to explore the relative reactivity of these two moieties when connected through linkers of various sizes, as well as the influence of the chain length.

■ RESULTS AND DISCUSSION

Chemistry. Colchicine was first converted into its deacetyl derivative 13 (Scheme 1) according to a literature procedure.[23]

Scheme 1. Synthesis of Pironetin Analogue/Colchicine Hybrids 1−8[a]
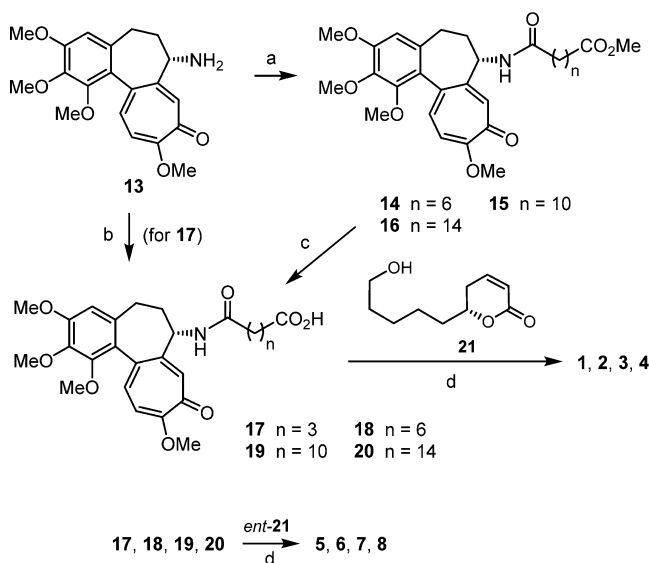
[a]Reagents and conditions: (a) MeO$_2$C(CH$_2$)$_n$COOH, DCC, DMAP, CH$_2$Cl$_2$, 3 h, rt (14, 73%; 15, 82%; 16, 76%); (b) glutaric anhydride, DMSO, NMM, 45 min, rt (84%); (c) LiOH, aq MeOH, 6 h, rt (18, 64%; 19, 73%; 20, 66%); (d) 17−20, 2,4,6-trichlorobenzoyl chloride, Et$_3$N, 5 h, rt, then addition of 21 or ent-21, DMAP, 1 h, rt (1, 43%; 2, 50%; 3, 45%; 4, 57%; 5, 44%; 6, 57%; 7, 55%; 8, 54%). Acronyms and abbreviations: DMAP, 4-(N,N-dimethylamino)pyridine; DCC, dicyclohexylcarbodiimide; DMSO, dimethyl sulfoxide; NMM, N-methylmorpholine.

N-Acyl derivative 17 was prepared from 13 as reported by means of treatment with glutaric anhydride.[23] Derivatives 18−20 were prepared through alkaline hydrolysis of methyl esters 14−16, obtained in turn by means of N-acylation of 13 under the conditions indicated in Scheme 1 (for details, see the Experimental Section). O-Acylation of the known dihydropyrone 21[24] with acids 17−20 under Yamaguchi conditions[25] afforded the desired compounds 1−4. Compounds 5−8 were prepared in the same way from dihydropyrone ent-21.[24]

The hybrid molecules 9−12 were prepared as depicted in Scheme 2. The known dihydropyrone 22[24] was esterified with acids 17−20 as above under Yamaguchi conditions. This yielded compounds 23−26, which were subjected to desilylation to furnish the desired 9−12.

After synthesis of the hybrid molecules was completed, the compounds were studied to determine their cytotoxic activity and their ability to disrupt the microtubule network.

Cytotoxicity Assays. We have carried out a measurement of the cytotoxicity of compounds 1−12. To do so, IC$_{50}$

Scheme 2. Synthesis of Pironetin Analogue/Colchicine Hybrids 9−12[a]
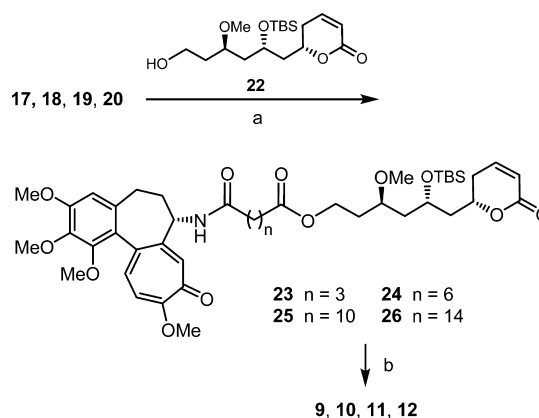
[a]Reagents and conditions: (a) 17−20, 2,4,6-trichlorobenzoyl chloride, Et$_3$N, 5 h, rt, then addition of 22, DMAP, 1 h, rt (23, 45%; 24, 43%; 25, 55%; 26, 46%); (b) 48% aq HF, MeCN, 3 h, rt (9, 67%; 10, 67%; 11, 74%; 12, 63%).

measurements were performed as described in the Experimental Section using two types of tumoral cells, the human colon adenocarcinoma (HT-29) and the breast adenocarcinoma (MCF-7) cell lines. For the sake of comparison, one nontumoral cell line, the human embryonic kidney cell line (HEK-293),[26] was employed in the assays. The cytotoxicity values, expressed as the concentration (μmol/L) required to produce 50% inhibition of cell growth (IC$_{50}$), are shown in Table 1 together with the A and B coefficients, obtained by dividing the IC$_{50}$ values of the nontumoral cell line (HEK-293) by those of one or the other tumoral cell line (see footnotes [b] and [c] in the table). The higher the value of the A or B coefficient, the higher the therapeutic safety margin of the compound in the corresponding cell line.

The observed IC$_{50}$ values are in most cases in the medium to low micromolar range, thus making the compounds 2−3 orders of magnitude less cytotoxic than either colchicine or pironetin. For the HT-29 cell line, only compounds 4, 9, 10, and 12 showed a noticeable cytotoxicity in the low micromolar range. However, the A coefficient was in most cases very low; i.e., these compounds were similarly toxic for normal and HT-29 tumoral cells.

The situation was different in the case of the MCF-7 cell line, which showed a much higher sensitivity toward compounds 1−4, 7, and 8, already in the nanomolar range (IC$_{50}$ < 1 μM). Interestingly, the B coefficient was high in some cases (1, 2, and 7), which indicates a better safety margin for these compounds than in the case of the HT-29 line. However, it is not easy to draw solid conclusions about the relation between the structures and the observed cytotoxicity. Within the subsets of hybrid molecules where there are differences in the carbon chain length (e.g., 1−4, 5−8, and 9−12), the IC$_{50}$ values are similar and do not show a clear relation with the length of the carbon chain. No explanation for this fact can be proposed without knowing whether these compounds are interacting with tubulin at the pironetin site (irreversible covalent binding to α-tubulin) or at the colchicine site (reversible noncovalent binding to β-tubulin). Experiments in this direction will be discussed below.

Indirect Immunofluorescence and Cell Cycle. To establish the cellular mechanisms of action of the compounds,

Table 1. Cytotoxicity of Pironetin Analogue/Colchicine Hybrids 1−12 toward Two Tumoral (HT-29 and MCF-7) Cell Lines and One Normal (HEK-293) Cell Line[a]

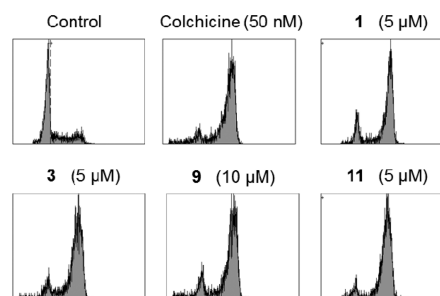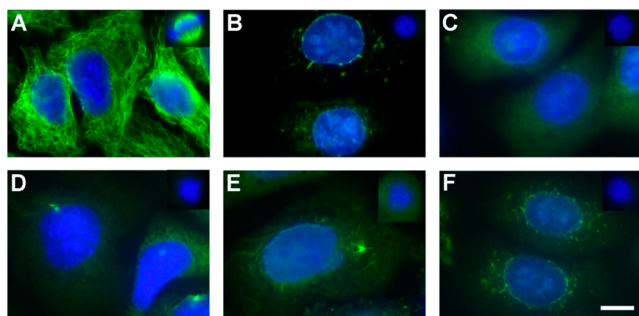| drug	HT-29	MCF-7	HEK-293	A^b	B^c
colchicine	0.050 ± 0.003	0.012 ± 0.007	0.005 ± 0.001	0.1	0.4
pironetin	0.0064 ± 0.0007	0.006 ± 0.002	0.017 ± 0.001	2.6	2.8
1	21 ± 6	0.7 ± 0.2	6 ± 2	0.3	8.7
2	20 ± 8	0.29 ± 0.24	33 ± 4	1.6	>100
3	18 ± 3	0.33 ± 0.18	1.40 ± 0.95	<0.1	4.2
4	8 ± 5	0.6 ± 0.3	0.44 ± 0.09	<0.1	0.7
5	65 ± 15	19 ± 1	0.4 ± 0,3	<0.1	<0.1
6	40 ± 6	12 ± 5	0.7 ± 0.2	<0.1	<0.1
7	40 ± 6	0.3 ± 0.2	24 ± 10	0.6	80
8	30 ± 19	0.5 ± 0.1	0.5 ± 0.1	<0.1	1
9	7 ± 1	36 ± 7	14 ± 3	2	0.4
10	3.8 ± 0.7	9 ± 3	7 ± 1	1.8	0.7
11	31 ± 11	60 ± 1	3.8 ± 0.6	0.1	<0.1
12	1.4 ± 0.8	28 ± 0.1	2 ± 1	1.6	<0.1

[a]IC_{50} values, which include those of the parent compounds colchicine and pironetin, are expressed as the compound concentration (μmol/L or μM) that causes 50% inhibition of cell growth. The values are the average (±SD) of three different measurements performed as described in the Experimental Section. [b]$A = IC_{50}(HEK-293)/IC_{50}(HT-29)$. [c]$B = IC_{50}(HEK-293)/IC_{50}(MCF-7)$.

we studied their effect on the microtubule cytoskeleton. Among the 12 available compounds, ligands **1**, **3**, **9**, and **11** were considered to be appropriate representatives of the whole group because they differ in the type of pironetin moiety (with either one or three stereocenters) and/or the length of the spacer carbon chain (either a short one, $n = 3$, or a long one, $n = 10$). Therefore, we selected them for this and the subsequent biological experiments. Compounds with the longest carbon chain ($n = 14$) were not easy to manipulate because of their very high hydrophobicity and consequently low solubility. For that reason, they were not used in these experiments. Compounds **5−8** were not selected either, because in general they did not perform better in cytotoxicity than **1−4**.

For the study of the effect on the microtubule cytoskeleton, we used non-small-cell lung adenocarcinoma cells (A-549),[27] which were incubated for 24 h in the presence of colchicine and compounds **1**, **3**, **9**, and **11** (Figure 5). Colchicine at 50 nM concentration almost completely depolymerizes cellular microtubules (D). Compounds **1** (B) and **11** (F) displayed at 1 μM concentration a similar effect in microtubule depolymerization;

Figure 5. Effect of hybrid compounds **1**, **3**, **9**, and **11** as compared to colchicine on the microtubule network and the nucleus morphology. A549 cells were incubated for 24 h with drug vehicle DMSO (A), 1 μM **1** (B), 5 μM **3** (C), 50 nM colchicine (D), 20 μM **9** (E), and 1 μM **11** (F). Microtubules were stained with α-tubulin antibodies, whereas DNA was stained with Hoechst 33342. Insets are mitotic spindles from the same preparation. The scale bar (F) represents 10 μm. All panels and insets have the same magnification.

i.e., they are 20 times less active than colchicine. Compounds **3** (C) and **9** (E) were visibly less active than **1** and **11**. In these preparations, metaphase mitotic cells with type IV mitotic spindles[28] were observed, with the DNA forming a ball without microtubules (insets in Figure 5). Aberrant mitoses were also present in all preparations.

We next studied whether compounds **1**, **3**, **9**, and **11** are able to block A549 cells in the G2/M phase of the cell cycle (Figure 6) in the same way as other microtubule-modulating agents do.

Figure 6. Cell cycle histograms of A549 lung carcinoma cells untreated (control) or treated with colchicine and compounds **1**, **3**, **9**, and **11**. The lowest ligand concentration that induces maximal arrest in the G2/M phase is depicted.

Thus, the cells were incubated for 20 h with the different ligands or the drug vehicle. Colchicine at 50 nM concentration arrested cells in the G2/M phase almost completely. All four compounds **1**, **3**, **9**, and **11** caused a similar effect at concentrations in the low micromolar range (≤10 μM), with **11** being somewhat more active. We may thus conclude that, although less cytotoxic than colchicine, these hybrid molecules also perturb the microtubular network and cause mitotic arrest in the G2/M phase (more than 80% of the cells are in this phase of the cell cycle).

Inhibition of Microtubule Assembly. The confirmation of cellular microtubule assembly inhibition activity by compounds **1**, **3**, **9**, and **11** led us to study their ability to inhibit purified tubulin microtubule assembly. We wished to know whether the activity is exerted by tubulin binding in the way pironetin does or in the way colchicine does. To do so, the

critical concentration[29] required for tubulin assembly was determined in glycerol-assembling buffer (GAB) in the presence of an excess (30 μM) of compounds **1**, **3**, **9**, and **11**. Indeed, the concentration of tubulin required to produce assembly increases from 3.30 $\pm$ 0.10 μM in the absence of ligands (DMSO vehicle) to a maximum value of 6.6 $\pm$ 1.1 μM in their presence, the latter being shown by compound **1** (Table 2). The other compounds (**3**, **9**, and **11**) showed

Table 2. Critical Concentration (CrC) for the Assembly of Purified Tubulin in GAB Proteins in the Presence of the Hybrid Ligands[a]

compd	CrC (μM)	compd	CrC (μM)
DMSO	3.30 $\pm$ 0.10	1	6.6 $\pm$ 1.1
docetaxel	0.9 $\pm$ 0.2	3	6.3 $\pm$ 0.7
pironetin	>15	9	5.3 $\pm$ 0.1
colchicine	>15	11	5.7 $\pm$ 0.3

[a]The concentration is 25 μM for docetaxel, colchicine, and pironetin and 30 μM for compounds **1**, **3**, **9**, and **11**. Data are the average of three measurements. Errors (SD) are standard errors of the average. The tubulin concentration is 20 μM in all experiments.

slightly lower values of the critical concentration, but it is anyway clear that all four ligands inhibit microtubule assembly. For the sake of comparison, the values measured for docetaxel (a microtubule-stabilizing agent), colchicine, and pironetin have been included. The values measured for the hybrid molecules confirm therefore that the observed effect in cells is due to their interaction with tubulin.

Mechanisms of Interaction of the Hybrid Molecules with Tubulin. With the idea of acquiring a more detailed view of the binding mechanism of these hybrid molecules, the effect of compounds **1**, **3**, **9**, and **11** on A2780 and A2780AD human ovarian carcinoma cells[30] was investigated. A2780 cells are sensitive to chemotherapy, whereas A2780AD cells have acquired resistance by means of P-glycoprotein overexpression. Thus, we determined the IC$_{50}$ values of the aforementioned compounds and compared them with those measured for pironetin and colchicine (Table 3). Pironetin is active in the low nanomolar range with similar values in both the parental and resistant cell lines, as expected for a compound with a mechanism of action based on covalent binding to its target.[30] Colchicine is also cytotoxic in the low nanomolar range for the

Table 3. Cytotoxicity of Several Selected Compounds toward Ovarian Carcinoma Cells Sensitive (A2780) and Resistant (A2780AD) to Chemotherapy[a]

drug	A2780	A2780AD	RF[b]
colchicine	0.015 $\pm$ 0.002	0.306 $\pm$ 0.34	>20
pironetin	0.008 $\pm$ 0.001	0.025 $\pm$ 0.002	~3
1	0.5 $\pm$ 0.001	59 $\pm$ 10	118
3	0.24 $\pm$ 0.002	26.5 $\pm$ 0.4	110
9	1.9 $\pm$ 0.1	>100	>50
11	0.4 $\pm$ 0.002	14.8 $\pm$ 0.1	~37

[a]IC$_{50}$ values, which include those of the parent compounds colchicine and pironetin, are expressed as the compound concentration (μmol/L or μM) that causes 50% inhibition of cell growth. The values are the average ($\pm$SD) of three different measurements performed as described in the Experimental Section. [b]Resistance factor, obtained by dividing the IC$_{50}$ of the A2780AD cell line by that of the parental A2780 line.

sensitive line, but the IC$_{50}$ value for the resistant line was noticeably higher (RF > 20), in accordance with that expected for a noncovalent binding mode. Table 3 shows that compounds **1**, **3**, **9**, and **11** are also very cytotoxic, most particularly **1**, **3**, and **11** (IC$_{50}$ = 500, 240, and 400 nM, respectively), but it is also worth mentioning that these four compounds exhibit high RF values, a feature which would suggest that they are binding to tubulin through a noncovalent mode. However, the large hydrophobic spacer may turn the substrates into good substrates for the P-glycoprotein. Since this would favor the resistance mechanism in the A2780AD cells, binding through the pironetin site cannot be discarded on the basis of these data alone.

To deepen our understanding of these interaction mechanisms, we have carried out measurements of the responses of tubulin critical concentration to changes in the concentrations of ligands. The results in the specific case of compound **11** and colchicine are shown in Table 4. In principle, a different

Table 4. Responses of the CrC Values to Changes in the Concentrations of Colchicine and Compound 11[a]

compd 11		colchicine	
concn (μM)	CrC (μM)	concn (μM)	CrC (μM)
DMSO (control)	3.3 $\pm$ 0.1	DMSO (control)	3.3 $\pm$ 0.1
0.1	3.4 $\pm$ 0.1	0.1	3.3 $\pm$ 0.1
0.5	3.5 $\pm$ 0.1	0.5	3.9 $\pm$ 0.1
1	4.0 $\pm$ 0.1	1	4.3 $\pm$ 0.1
5	4.5 $\pm$ 0.3	5	6.6 $\pm$ 0.7
10	5.9 $\pm$ 0.1	10	12.9 $\pm$ 1.0
30	5.7 $\pm$ 0.3	30	13.7 $\pm$ 3.3

[a]Data are the average of three measurements. Errors (SD) are standard errors of the average. The tubulin concentration is 20 μM in all experiments.

dependence of the inhibition of microtubule assembly on the ligand concentration would be expected depending on the way the ligand reacts with tubulin. On one hand, pironetin reacts covalently with the α subunit in the interdimer interface, where it will inhibit the addition of the modified tubulin dimer.[13d] The net result is a decrease of the concentration of free tubulin dimers available to bind to the microtubule end in a stoichiometric way. On the other hand, colchicine binds in the intradimer interface with the result of a change in the geometry of the dimer.[31] This modified dimer actually binds to the microtubule end but prevents the addition of further dimers, thus acting as a mitotic poison. Furthermore, dimers modified in this way are able to assemble with formation of a polymer with a different geometry. This implies that colchicine and its derivatives act at substoichiometric concentrations whereas pironetin acts in a stoichiometric way. As a consequence, for pironetin-type ligands, a continuous increment in the critical concentration required for assembly has to be expected when the drug concentration increases, leading to a nonassembly system when the pironetin concentration is stoichiometric with tubulin (all tubulin is unable to assembly). In contrast, a stabilization of the critical concentration measured would be expected for colchicine site ligands, when overstoichiometric concentrations are reached.

The observed results do not allow us to clearly distinguish between a stoichiometric type of inhibition (pironetin-like) and a poison type of inhibition (colchicine-like). This is probably due to the lower potency of the hybrid compounds as

compared with the parent compounds colchicine and pironetin. However, since the behavior of compound **11** at over-stoichiometric concentrations (30 μM for 20 μM tubulin) resembles that of colchicine, i.e., a stabilization of the critical concentration observed, it could perhaps be concluded that this compound binds to tubulin through the colchicine moiety. However, a more decisive conclusion is still lacking.

To check the binding mechanisms by means of another additional method, we investigated the direct interaction of ligands **1**, **3**, **9**, and **11** with tubulin. The method used was related to that employed in our former study[18a] to determine whether our analogues did actually compete with pironetin for binding to tubulin. Thus, we allowed each of the four compounds at 30 μM concentration to interact with tubulin at the same concentration and then extracted the solution with an organic solvent (see the Experimental Section for details). We then analyzed the fraction of the ligand (solution A) which was extracted with the solvent. Since interaction at the pironetin analogue side is expected to irreversibly lead to a covalent bond with tubulin, the corresponding molecules will not be extracted with the organic solvent. In contrast, interaction at the colchicine side is expected to lead to the reversible formation of a noncovalent bond, whereby the corresponding molecules will be extracted with the solvent.

In a second experiment, each of the four compounds at 30 μM concentration was allowed to interact as above with tubulin. After allowing for microtubule assembly, the suspension was ultracentrifuged, and the supernatant solution was separated from the solid pellet. Then both the solution and the pellet were separately extracted with the organic solvent. Material extracted from the supernatant solution (solution B) contains molecules that have not interacted with tubulin, whereas material extracted from the pellet (solution C) contains molecules that have interacted with tubulin in a noncovalent mode (colchicine end). Obviously, molecules that have become covalently bound to tubulin (pironetin end) remain in the pellet but are not extracted with the solvent.

Examination of the values in Table 5 suggests that compounds **1** and **9** interact only weakly with tubulin at the

Table 5. Interaction of Compounds 1, 3, 9, and 11 with Tubulin at Equimolecular Concentration

compd	concn[a] (μM)		
	solution A	solution B	solution C
1	21.7	18.1	5.7
3	6.9	2.0	5.7
9	28.5	20.5	4.7
11	12.8	7.3	3.4

[a]Concentration of the respective compound in the corresponding extract (reference solution in the absence of tubulin, 30 μM).

pironetin end, as indicated by the fact that most of the respective compound remains in solution A. The presence of the same compounds in low concentration in solution C indicates that some interaction, although not a strong one, has taken place at the colchicine end. As regards compounds **3** and **11**, they display a strong interaction at the pironetin end, most particularly **3**, as shown by the fact that only a small percentage of the respective compound remains in solution A. Both compounds also show interaction at the colchicine end with an intensity similar to that of the other two.

The aforementioned results have to be considered in light of the structures of the corresponding compounds. On one hand, molecules of compounds **1** and **9**, which interact weakly with tubulin through the pironetin end, display a short spacer between the latter and the colchicine end. It is thus possible that because of the steric bulk of the colchicine "tail", the molecule experiences a marked kinetic hurdle to penetrate through the binding channel at the pironetin site in α-tubulin. That the interaction with the colchicine end is also weak may possibly be due to the size of the *N*-acyl residue. Indeed, it has been reported that the activity of *N*-acyl derivatives of colchicine is dependent on the size of the substituent, with larger *N*-acyl residues giving rise to lower activities.[32] On the other hand, molecules of compounds **3** and **11**, which display a much longer spacer between the pironetin and the colchicine ends, do not find high steric barriers imposed by the now remote colchicine tail. As a result, they can covalently bind to the pironetin site. In any case, we cannot discard the alternative possibility that compound **3**, which has the simplest pironetin chain and is thus structurally much more distant from this natural product, is actually interacting covalently in a nonselective way with some unspecified nucleophilic residue of the protein chain not situated at the pironetin binding site.

The results presented above are worth discussing. While some of the data, such as the CrC values in Table 4 and most particularly the high RF values in Table 3, point to ligand−tubulin interactions taking place through the colchicine end, even though weakly, those of Table 5 indicate that binding may occur mainly at the pironetin end, provided that the length of the spacer is appropriate. A possible explanation for this discrepancy is related to the structures of ligands **1−12**. Half of the structure corresponds to an essentially unchanged colchicine moiety, whereas the other half displays a markedly simplified pironetin fragment. Our previous results[18] have shown that even minor modifications (deletions in our cases) of the pironetin moiety lead to decreases of the cytotoxic activity of about 2−3 orders of magnitude. Therefore, it is likely that the low cytotoxicities measured for compounds **1−12** with the cell lines in Table 1 are due mainly to the colchicine part, which interacts through the noncovalent mode. The responses of the CrC values to changes in concentrations (Table 4) point in the same direction. Covalent interactions though the pironetin end, such as those possibly occurring in molecules such as **3** and **11** (Table 5), are irreversible but may also be kinetically much slower than in the case of pironetin itself. In such a situation, the efflux mechanism mediated by the P-glycoprotein may have enough time to extrude the molecules in the case of resistant cells, therefore explaining the high RF values in Table 3.

■ CONCLUSION

We have prepared a set of synthetic hybrid molecules **1−12** containing a colchicine moiety and a fragment structurally related to the natural product pironetin. The two structural moieties have been connected through a spacer of variable length containing an ester and an amide group. The spacer was not long enough to permit simultaneous interaction of the molecules with the colchicine and the pironetin sites; thus, competitive binding was expected to take place. The cytotoxic activities of all these compounds and the interactions of some of them with tubulin have been investigated. While the tested compounds showed lower cytotoxicity values than the parental molecules colchicine and pironetin, we have found that the

binding of the compounds to tubulin is strongly influenced by the length of the connecting spacer. These results have been interpreted on the assumption that, if the distance between the pironetin and the colchicine ends is small (short spacer), the sterically bulky colchicine moiety hinders the hybrid molecules from arriving at the pironetin binding site. Consequently, reversible binding at the colchicine site takes place, even if with reduced activity. For longer spacers, steric hindrance to enter the pironetin site is lower, and the molecules may be able to bind covalently at that site.

■ EXPERIMENTAL SECTION

General Chemistry Methods. NMR spectra were measured at 25 °C. The signals of the deuterated solvent ($CDCl_3$) were taken as the reference. Multiplicity assignments of ^{13}C signals were made by means of the DEPT pulse sequence. Complete signal assignments in ^{1}H and ^{13}C NMR spectra with the aid of 2D homo- and heteronuclear pulse sequences (COSY, HSQC, HMBC) have been performed only for compounds **14** and **25**. In the remaining spectra, signals were assigned on the basis of the structural similarity (the positions and shapes of the NH signals have been found to vary to a marked extent depending on the concentration of the sample and perhaps also on the presence of water traces in the deuterated solvent). Electrospray high-resolution mass spectra (ESMS) were measured in the positive ion mode. IR data were measured with oily films on NaCl plates (oils) or KBr pellets (solids) and are given only for molecules with relevant functional groups (OH, C=O). Optical rotations were measured at 25 °C. Experiments which required an inert atmosphere were carried out under dry N_2 in flame-dried glassware. Et_2O and THF were freshly distilled from sodium/benzophenone ketyl and transferred via syringe. Dichloromethane was freshly distilled from CaH_2. Tertiary amines were freshly distilled from KOH. Commercially available reagents were used as received. Unless detailed otherwise, "workup" means pouring the reaction mixture into brine, followed by extraction with the solvent indicated in parentheses. If the reaction medium was acidic (basic), an additional washing with 5% aq $NaHCO_3$ (aq NH_4Cl) was performed. New washing with brine, drying over anhydrous Na_2SO_4, and elimination of the solvent under reduced pressure were followed by chromatography on a silica gel column (60–200 μm) with the indicated eluent. Where solutions were filtered through a Celite pad, the pad was additionally washed with the same solvent used, and the washings were incorporated into the main organic layer. The samples of compounds used for the biological studies were purified to >95% by means of preparative HPLC.

N-Acylation of Deacetylcolchicine (13) to Amide Esters 14–16 (Reaction Conditions a in Scheme 1). **13** (358 mg, ca. 1 mmol) and the appropriate diacid monomethyl ester (1.5 mmol) were dissolved under N_2 in dry CH_2Cl_2 (75 mL) and treated with DCC (1.55 g, 7.5 mmol) and DMAP (367 mg, 3 mmol). The mixture was then stirred for 3 h at room temperature and then filtered through Celite. The filtrate was evaporated under reduced pressure, and the residue was subjected to column chromatography on silica gel (CH_2Cl_2–MeOH, 98:2) to afford the desired compound **14–16**. For individual yields, see Scheme 1.

N-Acylation of 13 to Amide Acid 17 (Reaction Conditions b in Scheme 1). The reaction was performed under the reported conditions:[23] **13** (358 mg, 1 mmol) was dissolved under N_2 in dry DMSO (2 mL) and treated with glutaric anhydride (125 mg, 1.1 mol) and N-methylmorpholine (440 μL, 4 mmol). After being stirred at room temperature for 45 min, the reaction mixture was worked up (extraction with EtOAc). Column chromatography on silica gel (CH_2Cl_2–MeOH, 9:1) afforded compound **17** in 84% yield (yield and spectral data were not given in ref 23).

Alkaline Hydrolysis of Esters 14–16 to Acids 18–20 (Reaction Conditions c in Scheme 1). The appropriate ester **14–16** (2 mmol) was dissolved in MeOH (5 mL) at room temperature. After addition of a 5 M aqueous solution of NaOH (2 mL, 10 mmol), the reaction mixture was stirred for 8 h at room temperature. Workup (extraction with EtOAc) was followed by

column chromatography of the oily residue on silica gel (CH_2Cl_2–MeOH, 9:1) to afford the desired acid **18–20**. For individual yields, see Scheme 1.

Yamaguchi Esterification of Acids 17–20 with Pyrone Alcohol 21, ent-21, or 22 (Reaction Conditions d in Scheme 1 and a in Scheme 2). The appropriate acid **17–20** (0.5 mmol) was dissolved under N_2 in dry CH_2Cl_2 (10 mL) and treated sequentially with Et_3N (210 μL, 1.5 mmol) and 2,4,6-trichlorobenzoyl chloride (160 μL, ca. 1 mmol). The mixture was then stirred at room temperature for 5 h. Subsequently, a solution of the required alcohol **21**, ent-**21**, or **22** (1 mmol) and DMAP (122 mg, 1 mmol) in dry CH_2Cl_2 (5 mL) was added dropwise. The mixture was then further stirred at room temperature for 30 min. Workup (extraction with CH_2Cl_2) was followed by column chromatography of the oily residue on silica gel (first hexane–EtOAc (1:4), then CH_2Cl_2–MeOH (98:2)). This provided the desired esters **1–8** and **23–26**. For individual yields, see Scheme 2.

Acid-Catalyzed Desilylation of Compounds 23–26 to 9–12 (Reaction Conditions b in Scheme 2). The appropriate silylated compound (0.2 mmol) was dissolved in MeCN (2 mL) and treated with 48% aq HF (84 μL, ca. 2 mmol). The mixture was then stirred at room temperature for 3 h, cooled, and neutralized by addition of solid $NaHCO_3$. After filtration, the solution was evaporated under reduced pressure, and the oily residue was subjected to column chromatography on silica gel (EtOAc–MeOH, 6:4) to yield the desired desilylated compound. For individual yields, see Scheme 2.

Compounds are described in numerically increasing order.

Data for 5-[(2R)-6-oxo-3,6-dihydro-2H-pyran-2-yl]pentyl 5-oxo-5-{(7S)-1,2,3,10-tetramethoxy-9-oxo-5,6,7,9-tetrahydrobenzo[a]heptalen-7-yl]amino}pentanoate (1): oil; $[\alpha]_D$ −123.7 (c 0.79, $CHCl_3$); ^{1}H NMR (500 MHz) δ 7.43 (1H, s), 7.42 (1H, br s, NH), 7.26 (1H, d, J = 10.7 Hz), 6.85 (1H, ddd, J = 9.7, 5.4, 3 Hz), 6.81 (1H, d, J = 10.7 Hz), 6.50 (1H, s), 5.98 (1H, ddd, J = 9.7, 2.5, 1.5 Hz), 4.60 (1H, m), 4.41 (1H, m), 4.00 (2H, t, J = 6.6 Hz), 3.97 (3H, s), 3.90 (3H, s), 3.87 (3H, s), 3.63 (3H, s), 2.48 (1H, br dd, J ≈ 13.3, 6.3 Hz), 2.40–2.20 (8H, br m), 1.90–1.70 (4H, br m), 1.65–1.30 (7H, br m); ^{13}C NMR (125 MHz) δ 179.4, 173.1, 171.8, 164.5, 163.9, 153.4, 151.6, 151.1, 141.6, 136.4, 134.1, 125.6 (C), 145.1, 135.1, 130.6, 121.4, 112.3, 107.3, 77.7, 52.1 (CH), 64.1, 36.6, 34.9, 34.6, 33.5, 29.8, 29.2, 28.3, 25.6, 24.3, 20.6 (CH₂), 61.4, 61.2, 56.2, 56.0 (CH₃); IR ν_{max} 3300 br (NH), 1729 br, 1672 (C=O) cm^{-1}; HR ESMS m/z 638.2969 (M + H$^+$), calcd for $C_{35}H_{44}NO_{10}$, 638.2965.

Data for 5-[(2R)-6-oxo-3,6-dihydro-2H-pyran-2-yl]pentyl 8-oxo-8-{(7S)-1,2,3,10-tetramethoxy-9-oxo-5,6,7,9-tetrahydrobenzo[a]heptalen-7-yl]amino}octanoate (2): oil; $[\alpha]_D$ −136.8 (c 1.3, $CHCl_3$); ^{1}H NMR (500 MHz) δ 7.80 (1H, br d, J ≈ 7 Hz, NH), 7.42 (1H, s), 7.21 (1H, d, J = 10.7 Hz), 6.79 (2H, m), 6.44 (1H, s), 5.90 (1H, br d, J ≈ 9.8 Hz), 4.54 (1H, m), 4.34 (1H, m), 3.94 (2H, t, J = 6.7 Hz), 3.90 (3H, s), 3.84 (3H, s), 3.80 (3H, s), 3.57 (3H, s), 2.42 (1H, br dd, J ≈ 13.1, 6 Hz), 2.30–2.10 (7H, br m), 1.80 (1H, m), 1.69 (1H, m), 1.60–1.40 (8H, br m), 1.40–1.20 (8H, br m); ^{13}C NMR (125 MHz) δ 179.1, 173.4, 172.6, 164.3, 163.7, 153.1, 152.0, 150.9, 141.3, 136.4, 134.0, 125.4 (C), 145.1, 135.0, 130.4, 120.9, 112.3, 107.1, 77.5, 52.0 (CH), 63.7, 36.2, 35.6, 34.4, 33.9, 29.6, 29.0, 28.6, 28.4, 28.2, 25.4, 24.9, 24.4, 24.1 (CH₂), 61.2, 61.0, 56.1, 55.8 (CH₃); IR ν_{max} 3300 br (NH), 1725 br, 1674 (C=O) cm^{-1}; HR ESMS m/z 680.3436 (M + H$^+$), calcd for $C_{38}H_{50}NO_{10}$, 680.3435.

Data for 5-[(2R)-6-oxo-3,6-dihydro-2H-pyran-2-yl]pentyl 12-oxo-12-{(7S)-1,2,3,10-tetramethoxy-9-oxo-5,6,7,9-tetrahydrobenzo[a]heptalen-7-yl)amino}dodecanoate (3): oil; $[\alpha]_D$ −52 (c 1.4, $CHCl_3$); ^{1}H NMR (500 MHz) δ 7.45 (2H, br s), 7.26 (1H, d, J = 10.7 Hz), 6.82 (1H, overlapped m), 6.80 (1H, d, J = 10.7 Hz), 6.49 (1H, s), 5.97 (1H, br d, J ≈ 9.8 Hz), 4.60 (1H, m), 4.39 (1H, m), 4.01 (2H, t, J = 6.6 Hz), 3.95 (3H, s), 3.89 (3H, s), 3.84 (3H, s), 3.60 (3H, s), 2.46 (1H, br dd, J ≈ 13.2, 6.4 Hz), 2.35–2.10 (7H, br m), 1.85–1.70 (2H, m), 1.65–1.40 (8H, br m), 1.40–1.20 (16H, br m); ^{13}C NMR (125 MHz) δ 179.3, 173.7, 172.8, 164.3, 163.8, 153.3, 151.9, 151.0, 141.5, 136.5, 134.1, 125.6 (C), 145.0, 135.0, 130.5, 121.2, 112.4, 107.3, 77.7, 52.0 (CH), 63.9, 36.5, 36.0, 34.6, 34.2, 29.8, 29.3 (×2), 29.2 (×2), 29.1, 29.0, 28.9, 28.4, 25.6, 25.2, 24.9, 24.3 (CH₂), 61.4, 61.2, 56.2, 55.9 (CH₃); IR ν_{max} 3300 br (NH), 1725 br, 1672

(C=O) cm^{-1}; HR ESMS m/z 736.4056 (M + H$^+$), calcd for C$_{42}$H$_{58}$NO$_{10}$, 736.4061.

Data for 5-[(2R)-6-oxo-3,6-dihydro-2H-pyran-2-yl]pentyl 16-oxo-16-{(7S)-1,2,3,10-tetramethoxy-9-oxo-5,6,7,9-tetrahydrobenzo[a]heptalen-7-yl)amino}hexadecanoate (4): oil; [α]$_D$ −88.7 (c 1.4, CHCl$_3$); ^{1}H NMR (500 MHz) δ 7.45 (1H, s), 7.28 (1H, d, J = 10.7 Hz), 7.20 (1H, br d, J ≈ 7 Hz, NH), 6.86 (1H, ddd, J = 9.8, 5.5, 3.5 Hz), 6.81 (1H, d, J = 10.7 Hz), 6.50 (1H, s), 5.99 (1H, br d, J ≈ 9.8 Hz), 4.62 (1H, m), 4.40 (1H, m), 4.03 (2H, t, J = 6.6 Hz), 3.97 (3H, s), 3.91 (3H, s), 3.87 (3H, s), 3.62 (3H, s), 2.48 (1H, br dd, J ≈ 13.6, 6.3 Hz), 2.40−2.15 (7H, br m), 1.85−1.70 (2H, m), 1.65−1.50 (10H, br m), 1.45−1.20 (22H, br m); ^{13}C NMR (125 MHz) δ 179.3, 173.7, 172.9, 164.3, 163.8, 153.3, 151.9, 151.0, 141.5, 136.5, 134.1, 125.6 (C), 145.0, 135.0, 130.5, 121.2, 112.4, 107.3, 77.7, 52.0 (CH), 63.9, 36.5, 36.0, 34.6, 34.2, 29.8, 29.4 (×5), 29.3 (×4), 29.1, 29.0, 28.4, 25.6, 25.3, 24.9, 24.3 (CH$_2$), 61.4, 61.2, 56.2, 56.0 (CH$_3$); IR ν$_{max}$ 3300 br (NH), 1731 br, 1672 (C=O) cm^{-1}; HR ESMS m/z 792.4691 (M + H$^+$), calcd for C$_{46}$H$_{66}$NO$_{10}$, 792.4687.

Data for 5-[(2S)-6-oxo-3,6-dihydro-2H-pyran-2-yl]pentyl 5-oxo-5-{(7S)-1,2,3,10-tetramethoxy-9-oxo-5,6,7,9-tetrahydrobenzo[a]heptalen-7-yl)amino}pentanoate (5): oil; [α]$_D$ −54.7 (c 1.24, CHCl$_3$); ^{1}H NMR (500 MHz) δ 7.66 (1H, br d, J ≈ 7 Hz, NH), 7.40 (1H, s), 7.22 (1H, d, J = 10.7 Hz), 6.81 (1H, overlapped m), 6.79 (1H, d, J = 10.7 Hz), 6.46 (1H, s), 5.91 (1H, br d, J ≈ 9.8 Hz), 4.55 (1H, m), 4.34 (1H, m), 3.94 (2H, t, J = 6.6 Hz), 3.92 (3H, s), 3.85 (3H, s), 3.81 (3H, s), 3.58 (3H, s), 2.44 (1H, br dd, J ≈ 13.3, 6.2 Hz), 2.30−2.10 (7H, br m), 1.85−1.65 (4H, br m), 1.60−1.25 (8H, br m); ^{13}C NMR (125 MHz) δ 179.2, 172.9, 171.8, 164.4, 163.7, 153.2, 151.7, 150.9, 141.4, 136.3, 134.1, 125.4 (C), 145.1, 135.0, 130.4, 121.0, 112.3, 107.2, 77.7, 52.0 (CH), 63.9, 36.3, 34.6, 34.4, 33.3, 29.7, 29.1, 28.1, 25.5, 24.2, 20.4 (CH$_2$), 61.2, 61.0, 56.1, 55.9 (CH$_3$); IR ν$_{max}$ 3300 br (NH), 1722 br, 1672 (C=O) cm^{-1}; HR ESMS m/z 638.2969 (M + H$^+$), calcd for C$_{35}$H$_{44}$NO$_{10}$, 638.2965.

Data for 5-[(2S)-6-oxo-3,6-dihydro-2H-pyran-2-yl]pentyl 8-oxo-8-{(7S)-1,2,3,10-tetramethoxy-9-oxo-5,6,7,9-tetrahydrobenzo[a]heptalen-7-yl)amino}octanoate (6): oil; [α]$_D$ −69.8 (c 0.8, CHCl$_3$); ^{1}H NMR (500 MHz) δ 7.46 (1H, s), 7.43 (1H, br d, J ≈ 7 Hz, NH), 7.27 (1H, d, J = 10.7 Hz), 6.84 (1H, ddd, J = 9.7, 5.4, 3 Hz), 6.81 (1H, d, J = 10.7 Hz), 6.50 (1H, s), 5.97 (1H, br dt, J ≈ 9.8, 2 Hz), 4.60 (1H, m), 4.38 (1H, m), 4.00 (2H, t, J = 6.6 Hz), 3.96 (3H, s), 3.89 (3H, s), 3.85 (3H, s), 3.61 (3H, s), 2.47 (1H, br dd, J ≈ 13.4, 6 Hz), 2.40−2.10 (7H, br m), 1.84 (1H, m), 1.75 (1H, m), 1.65−1.45 (8H, br m), 1.40−1.20 (8H, br m); ^{13}C NMR (125 MHz) δ 179.3, 173.6, 172.6, 164.4, 163.8, 153.3, 151.8, 151.0, 141.5, 136.5, 134.1, 125.6 (C), 145.1, 135.0, 130.6, 121.2, 112.4, 107.3, 77.7, 52.0 (CH), 63.9, 36.5, 35.8, 34.6, 34.0, 29.8, 29.2, 28.8, 28.6, 28.4, 25.6, 25.1, 24.6, 24.3 (CH$_2$), 61.4, 61.2, 56.2, 56.0 (CH$_3$); IR ν$_{max}$ 3300 br (NH), 1721 br, 1674 (C=O) cm^{-1}; HR ESMS m/z 680.3433 (M + H$^+$), calcd for C$_{38}$H$_{50}$NO$_{10}$, 680.3435.

Data for 5-[(2S)-6-oxo-3,6-dihydro-2H-pyran-2-yl]pentyl 12-oxo-12-{(7S)-1,2,3,10-tetramethoxy-9-oxo-5,6,7,9-tetrahydrobenzo[a]heptalen-7-yl)amino}dodecanoate (7): oil; [α]$_D$ −22.2 (c 1.1, CHCl$_3$); ^{1}H NMR (500 MHz) δ 7.45 (1H, s), 7.30 (1H, d, J = 10.7 Hz), 6.88 (1H, ddd, J = 9.8, 5.4, 3 Hz), 6.85 (1H, d, J = 10.7 Hz), 6.70 (1H, br d, J ≈ 7 Hz, NH), 6.50 (1H, s), 6.01 (1H, br d, J ≈ 9.8 Hz), 4.62 (1H, m), 4.42 (1H, m), 4.04 (2H, t, J = 6.6 Hz), 3.98 (3H, s), 3.90 (3H, s), 3.86 (3H, s), 3.63 (3H, s), 2.46 (1H, br dd, J ≈ 13.2, 6.7 Hz), 2.40−2.10 (7H, br m), 1.83 (1H, m), 1.65−1.40 (9H, br m), 1.40−1.20 (16H, br m); ^{13}C NMR (125 MHz) δ 179.4, 173.9, 172.7, 164.4, 164.0, 153.4, 151.3, 151.2, 141.7, 136.3, 134.1, 125.7 (C), 145.0, 135.0, 130.7, 121.4, 112.3, 107.4, 77.8, 52.0 (CH), 64.0, 36.9, 36.3, 34.6, 34.7, 34.3, 34.0, 29.4, 29.3−29.0 (five partially overlapped signals), 28.5, 25.7, 25.4, 25.0, 24.5 (CH$_2$), 61.5, 61.3, 56.3, 56.1 (CH$_3$); IR ν$_{max}$ 3300 br (NH), 1734 br, 1671 (C=O) cm^{-1}; HR ESMS m/z 736.4062 (M + H$^+$), calcd for C$_{42}$H$_{58}$NO$_{10}$, 736.4061.

Data for 5-[(2S)-6-oxo-3,6-dihydro-2H-pyran-2-yl]pentyl 16-oxo-16-{(7S)-1,2,3,10-tetramethoxy-9-oxo-5,6,7,9-tetrahydrobenzo[a]heptalen-7-yl)amino}hexadecanoate (8): oil; [α]$_D$ −25.2 (c 1.9, CHCl$_3$); ^{1}H NMR (500 MHz) δ 7.46 (1H, s), 7.45 (1H, br d, J ≈ 7 Hz, NH), 7.28 (1H, d, J = 10.7 Hz), 6.84 (1H, ddd, J = 9.8, 5.4, 3 Hz), 6.82 (1H, d, J = 10.7 Hz), 6.49 (1H, s), 5.98

(1H, br d, J ≈ 9.8 Hz), 4.62 (1H, m), 4.38 (1H, m), 4.02 (2H, t, J = 6.6 Hz), 3.96 (3H, s), 3.90 (3H, s), 3.86 (3H, s), 3.62 (3H, s), 2.46 (1H, br dd, J ≈ 13.6, 6.4 Hz), 2.40−2.15 (7H, br m), 1.85−1.70 (2H, m), 1.65−1.50 (9H, br m), 1.40−1.20 (24H, br m); ^{13}C NMR (125 MHz) δ 179.3, 173.7, 172.9, 164.3, 163.8, 153.3, 151.9, 151.0, 141.5, 136.5, 134.1, 125.6 (C), 145.0, 135.0, 130.5, 121.2, 112.3, 107.3, 77.7, 52.0 (CH), 63.9, 36.5, 36.1, 34.6, 34.2, 29.8, 29.5 (×4), 29.4, 29.3 (×2), 29.2 (×2), 29.1, 29.0, 28.4, 25.6, 25.3, 24.9, 24.3 (CH$_2$), 61.5, 61.2, 56.2, 56.0 (CH$_3$); IR ν$_{max}$ 3300 br (NH), 1731 br, 1673 (C=O) cm^{-1}; HR ESMS m/z 792.4686 (M + H$^+$), calcd for C$_{46}$H$_{66}$NO$_{10}$, 792.4687.

Data for (3R,5S)-5-hydroxy-3-methoxy-6-[(2S)-6-oxo-3,6-dihydro-2H-pyran-2-yl]hexyl 5-oxo-5-{(7S)-(1,2,3,10-tetramethoxy-9-oxo-5,6,7,9-tetrahydrobenzo[a]heptalen-7-yl)amino}pentanoate (9): oil; [α]$_D$ +5.1 (c 0.3, CHCl$_3$); ^{1}H NMR (500 MHz) δ 7.44 (1H, s), 7.30 (1H, d, J = 10.8 Hz), 7.20 (1H, br d, J ≈ 7 Hz, NH), 6.86 (1H, ddd, J = 9.7, 5.5, 2.5 Hz), 6.84 (1H, d, J = 10.8 Hz), 6.53 (1H, s), 5.98 (1H, br d, J ≈ 9.8 Hz), 4.81 (1H, m), 4.65 (1H, m), 4.25 (2H, m), 4.15 (1H, m), 3.96 (3H, s), 3.93 (3H, s), 3.90 (3H, s), 3.67 (1H, m), 3.65 (3H, s), 3.30 (3H, s), 2.50 (1H, br dd, J ≈ 13.7, 6.3 Hz), 2.45−2.20 (9H, br m), 2.00−1.80 (7H, br m), 1.75−1.60 (2H, m); ^{13}C NMR (125 MHz) δ 179.5, 173.3, 171.9, 164.6, 164.0, 153.5, 152.0, 151.1, 141.7, 136.7, 134.3, 125.6 (C), 145.6, 135.3, 130.8, 121.2, 112.7, 107.4, 75.5, 75.0, 64.1, 52.0 (CH), 61.0, 43.1, 40.4, 36.8, 34.9, 33.6, 32.1, 29.9, 29.7, 20.8 (CH$_2$), 61.5, 61.3, 56.3, 56.1 (×2) (CH$_3$); IR ν$_{max}$ 3300 br (OH, NH), 1730 br, 1656 (C=O) cm^{-1}; HR ESMS m/z 698.3181 (M + H$^+$), calcd for C$_{37}$H$_{48}$NO$_{12}$, 698.3177.

Data for (3R,5S)-5-hydroxy-3-methoxy-6-[(2S)-6-oxo-3,6-dihydro-2H-pyran-2-yl]hexyl 8-oxo-8-{(7S)-(1,2,3,10-tetramethoxy-9-oxo-5,6,7,9-tetrahydrobenzo[a]heptalen-7-yl)amino}octanoate (10): oil; [α]$_D$ −106.6 (c 0.37, CHCl$_3$); ^{1}H NMR (500 MHz) δ 7.38 (1H, s), 7.29 (1H, d, J = 10.7 Hz), 6.89 (1H, ddd, J = 9.7, 5.5, 3 Hz), 6.82 (1H, d, J = 10.7 Hz), 6.54 (1H, s), 6.50 (1H, br d, J ≈ 7 Hz, NH), 6.02 (1H, ddd, J = 9.7, 2.5, 1 Hz), 4.80 (1H, m), 4.63 (1H, m), 4.26 (1H, m), 4.20−4.10 (2H, br m), 3.98 (3H, s), 3.94 (3H, s), 3.89 (3H, s), 3.65 (3H, s), 3.63 (1H, m), 3.37 (3H, s), 2.52 (1H, br dd, J ≈ 13.7, 6.3 Hz), 2.50−2.20 (5H, br m), 2.00−1.70 (5H, br m), 1.65−1.40 (10H, br m), 1.35−1.20 (4H, br m); ^{13}C NMR (125 MHz) δ 179.5, 173.7, 172.6, 164.6, 164.0, 153.5, 151.3, 151.2, 141.8, 136.4, 134.1, 125.7 (C), 145.5, 135.1, 130.8, 121.4, 112.3, 107.4, 76.2, 75.1, 64.3, 52.0 (CH), 60.9, 43.1, 40.4, 37.0, 36.2, 34.2, 32.3, 30.1, 29.9, 28.8, 28.6, 25.2, 24.7 (CH$_2$), 61.6, 61.4, 56.8, 56.3, 56.2 (CH$_3$); IR ν$_{max}$ 3300 br (OH, NH), 1724 br, 1673 (C=O) cm^{-1}; HR ESMS m/z 740.3649 (M + H$^+$), calcd for C$_{40}$H$_{54}$NO$_{12}$Si, 740.3646.

Data for (3R,5S)-5-hydroxy-3-methoxy-6-[(2S)-6-oxo-3,6-dihydro-2H-pyran-2-yl]hexyl 12-oxo-12-{(7S)-(1,2,3,10-tetramethoxy-9-oxo-5,6,7,9-tetrahydrobenzo[a]heptalen-7-yl)amino}dodecanoate (11): oil; [α]$_D$ −19 (c 0.14, CHCl$_3$); ^{1}H NMR (500 MHz) δ 7.37 (1H, s), 7.28 (1H, d, J = 10.7 Hz), 6.90 (1H, ddd, J = 9.7, 5.5, 2.5 Hz), 6.81 (1H, d, J = 10.7 Hz), 6.53 (1H, s), 6.40 (1H, br d, J ≈ 7 Hz, NH), 6.03 (1H, dt, J = 9.8, 1.5 Hz), 4.77 (1H, m), 4.66 (1H, m), 4.27 (1H, br t, J ≈ 9.5 Hz), 4.17 (2H, t, J = 6.6 Hz), 3.98 (3H, s), 3.95 (3H, s), 3.91 (3H, s), 3.66 (3H, s), 3.60 (1H, m), 3.37 (3H, s), 3.30 (1H, br s, OH), 2.52 (1H, br dd, J ≈ 13.3, 6.3 Hz), 2.45−2.15 (8H, br m), 2.00 (1H, m), 1.90−1.50 (10H, br m), 1.35−1.20 (12H, br m); ^{13}C NMR (125 MHz) δ 179.4, 173.8, 172.7, 164.4, 164.0, 153.4, 151.3, 151.2, 141.7, 136.3, 134.1, 125.7 (C), 145.3, 135.1, 130.7, 121.4, 112.3, 107.4, 76.5, 75.0, 64.4, 52.0 (CH), 60.9, 43.0, 39.9, 37.0, 36.4, 34.3, 32.4, 30.0, 29.9, 29.3−29.0 (six partially overlapped signals), 25.3, 24.9 (CH$_2$), 61.5, 61.3, 57.0, 56.3, 56.1 (CH$_3$); IR ν$_{max}$ 3300 br (OH, NH), 1737 br, 1674 (C=O) cm^{-1}; HR ESMS m/z 796.4276 (M + H$^+$), calcd for C$_{44}$H$_{62}$NO$_{12}$, 796.4272.

Data for (3R,5S)-5-hydroxy-3-methoxy-6-[(2S)-6-oxo-3,6-dihydro-2H-pyran-2-yl]hexyl 16-oxo-16-{(7S)-(1,2,3,10-tetramethoxy-9-oxo-5,6,7,9-tetrahydrobenzo[a]heptalen-7-yl)amino}hexadecanoate (12): oil; [α]$_D$ −59 (c 0.4, CHCl$_3$); ^{1}H NMR (500 MHz) δ 7.40 (1H, s), 7.29 (1H, d, J = 10.7 Hz), 6.89 (1H, ddd, J = 9.7, 5.4, 3 Hz), 6.82 (1H, d, J = 10.7 Hz), 6.60 (1H, br d, J ≈ 7 Hz, NH), 6.52 (1H, s), 6.02 (1H, ddd, J = 9.7, 2.5, 1.5 Hz), 4.76 (1H, m), 4.66 (1H, m), 4.28 (1H, br t, J ≈ 9.5 Hz), 4.16 (2H, t, J = 6.6 Hz), 3.98 (3H, s), 3.95 (3H, s), 3.90 (3H, s), 3.64 (3H, s), 3.60 (1H, m), 3.37

(3H, s), 3.30 (1H, br s, OH), 2.52 (1H, br dd, $J \approx 13.3$, 6.3 Hz), 2.45−2.20 (8H, br m), 1.99 (1H, m), 1.85−1.50 (10H, br m), 1.35−1.20 (20H, br m); ^{13}C NMR (125 MHz) δ 179.4, 173.8, 172.7, 164.4, 164.0, 153.4, 151.3, 151.2, 141.7, 136.3, 134.1, 125.7 (C), 145.3, 135.1, 130.7, 121.4, 112.3, 107.4, 76.5, 75.0, 64.4, 52.0 (CH), 60.9, 43.0, 39.9, 37.0, 36.4, 34.3, 32.4, 30.0, 29.9, 29.5−29.0 (10 partially overlapped signals), 25.4, 24.9 (CH$_2$), 61.5, 61.3, 57.0, 56.3, 56.1 (CH$_3$); IR ν_{max} 3300 br (OH, NH), 1727 br, 1671 (C=O) cm^{-1}; HR ESMS m/z 852.4896 (M + H$^+$), calcd for C$_{48}$H$_{70}$NO$_{12}$, 852.4898.

Data for methyl 8-oxo-8-[(7S)-(1,2,3,10-tetramethoxy-9-oxo-5,6,7,9-tetrahydrobenzo[a]heptalen-7-yl)amino]-octanoate (14): oil; $[\alpha]_D$ −119.3 (c 2, CHCl$_3$); ^{1}H NMR (500 MHz) δ 7.65 (1H, br d, $J \approx 7$ Hz, NH), 7.49 (1H, s, H-8), 7.28 (1H, d, $J = 10.5$ Hz, H-12), 6.83 (1H, d, $J = 10.5$ Hz, H-11), 6.50 (1H, s, H-4), 4.60 (1H, br dt, $J \approx 11.5$, 7 Hz, H-7), 3.96 (3H, s, 10-OMe), 3.90 (3H, s, 2-OMe), 3.85 (3H, s, 3-OMe), 3.62 (3H, s, 1-OMe), 3.59 (3H, s, ester OMe), 2.46 (1H, br dd, $J = 13.8$, 6.5 Hz, H-5α or H-5β), 2.34 (1H, br td, $J \approx 13.5$, 6.5 Hz, H-5β or H-5α), 2.30−2.10 (5H, br m, H-6α or H-6β, H-2′, H-7′), 1.84 (1H, m, H-6α or H-6β), 1.50−1.40 (4H, br m, H-3′, H-6′), 1.25−1.20 (4H, br m, H-4′, H-5′); ^{13}C NMR (125 MHz) δ 179.5 (C-9), 174.1 (C-8′), 172.7 (C-1′), 163.9 (C-10), 153.4 (C-3), 152.1 (C-7a), 151.1 (C-1), 141.6 (C-2), 136.6 (C-12a), 135.2 (C-12), 134.2 (C-4a), 130.5 (C-8), 125.6 (C-12b), 112.5 (C-11), 107.3 (C-4), 61.5 (1-OMe), 61.2 (2-OMe), 56.3 (10-OMe), 56.0 (3-OMe), 52.1 (C-7), 51.3 (ester OMe), 36.5 (C-6), 35.8 (C-2′), 33.8 (C-7′), 29.8 (C-5), 28.8, 28.6, 25.1, 24.6 (C-3′ to C-6′); IR ν_{max} 3300 br (NH), 1735 br, 1671, 1654 (C=O) cm^{-1}; HR ESMS m/z 528.2599 (M + H$^+$), calcd for C$_{29}$H$_{38}$NO$_8$, 528.2597. NMR signals of this compound were assigned with the aid of 2D homo- and heteronuclear pulse sequences (COSY, HSQC, HMBC). For atom numbering see the Supporting Information. Signal assignments within the colchicine fragment were consistent with literature data for colchicine.[33]

Data for methyl 12-oxo-12-[(7S)-(1,2,3,10-tetramethoxy-9-oxo-5,6,7,9-tetrahydrobenzo[a]heptalen-7-yl)amino]-dodecanoate (15): oil; $[\alpha]_D$ −55 (c 0.9, CHCl$_3$); ^{1}H NMR (500 MHz) δ 7.49 (1H, s), 7.48 (1H, br s, NH), 7.29 (1H, d, $J = 10.5$ Hz), 6.83 (1H, d, $J = 10.5$ Hz), 6.50 (1H, s), 4.62 (1H, m), 3.98 (3H, s), 3.91 (3H, s), 3.86 (3H, s), 3.62 (3H, s), 3.61 (3H, s), 2.47 (1H, br dd, $J \approx 13.3$, 6.4 Hz), 2.35 (1H, br td, $J \approx 13.3$, 6.7 Hz), 2.30−2.10 (5H, br m), 1.83 (1H, m), 1.60−1.45 (4H, br m), 1.35−1.20 (12H, br m); ^{13}C NMR (125 MHz) δ 179.5, 174.2, 172.7, 163.9, 153.4, 152.1, 151.1, 141.6, 136.6, 134.2, 125.6 (C), 135.2, 130.5, 112.5, 107.3, 52.1 (CH), 36.6, 36.0, 34.0, 29.9, 29.3−29.0 (six partially overlapped signals), 25.3, 24.8 (CH$_2$), 61.5, 61.3, 56.3, 56.0, 51.3 (CH$_3$); IR ν_{max} 3300 br (NH), 1736 br, 1674 (C=O) cm^{-1}; HR ESMS m/z 584.3229 (M + H$^+$), calcd for C$_{33}$H$_{46}$NO$_8$, 584.3223.

Data for methyl 16-oxo-16-[(7S)-(1,2,3,10-tetramethoxy-9-oxo-5,6,7,9-tetrahydrobenzo[a]heptalen-7-yl)amino]-hexadecanoate (16): oil; $[\alpha]_D$ −81.1 (c 1.3, CHCl$_3$); ^{1}H NMR (500 MHz) δ 8.00 (1H, br d, $J \approx 6.5$ Hz, NH), 7.49 (1H, s), 7.24 (1H, d, $J = 10.7$ Hz), 6.80 (1H, d, $J = 10.7$ Hz), 6.44 (1H, s), 4.56 (1H, m), 3.92 (3H, s), 3.85 (3H, s), 3.80 (3H, s), 3.57 (3H, s), 3.56 (3H, s), 2.40 (1H, br dd, $J \approx 13$, 6 Hz), 2.30 (1H, br td, $J \approx 13$, 6.4 Hz), 2.20−2.10 (5H, br m), 1.80 (1H, m), 1.55−1.40 (4H, br m), 1.30−1.15 (20H, br m); ^{13}C NMR (125 MHz) δ 179.2, 174.0, 172.8, 163.7, 153.2, 152.3, 150.9, 141.4, 136.6, 134.1, 125.4 (C), 135.1, 130.4, 112.5, 107.1, 52.0 (CH), 36.2, 35.8, 33.8, 29.7, 29.3−28.8 (10 partially overlapped signals), 25.2, 24.7 (CH$_2$), 61.3, 61.0, 56.1, 55.8, 51.1 (CH$_3$); IR ν_{max} 3300 br (NH), 1727 br, 1671 (C=O) cm^{-1}; HR ESMS m/z 640.3845 (M + H$^+$), calcd for C$_{37}$H$_{54}$NO$_8$, 640.3849.

Data for 5-oxo-5-[(7S)-(1,2,3,10-tetramethoxy-9-oxo-5,6,7,9-tetrahydrobenzo[a]heptalen-7-yl)amino)pentanoic acid (17): oil; $[\alpha]_D$ −110.9 (c 1.1, CHCl$_3$); ^{1}H NMR (500 MHz) δ 8.10 (1H, br d, $J \approx 6.5$ Hz, NH), 7.80 (1H, br s), 7.42 (1H, d, $J = 10.8$ Hz), 6.97 (1H, d, $J = 10.8$ Hz), 6.55 (1H, s), 4.65 (1H, m), 4.00 (3H, s), 3.94 (3H, s), 3.90 (3H, s), 3.64 (3H, s), 2.52 (1H, br dd, $J = 13.8$, 6.4 Hz), 2.45−2.20 (6H, br m), 2.05−1.90 (3H, br m) (carboxyl proton signal not detected); ^{13}C NMR (125 MHz) δ 179.4, 176.1*, 172.8, 164.0, 153.7, 153.5, 151.2, 141.6, 137.8, 134.4, 125.4 (C), 136.3, 130.9, 114.1,

107.5, 52.8 (CH), 36.0, 34.3, 33.3*, 30.0, 20.8 (CH$_2$), 61.6, 61.3, 56.5, 56.2 (CH$_3$) (asterisked signals are low and broad); IR ν_{max} 3300−2500 br (COOH, NH), 1713 br, 1660 (C=O) cm^{-1}; HR ESMS m/z 472.1972 (M + H$^+$), calcd for C$_{25}$H$_{30}$NO$_8$, 472.1971.

Data for 8-oxo-8-[(7S)-(1,2,3,10-tetramethoxy-9-oxo-5,6,7,9-tetrahydrobenzo[a]heptalen-7-yl)amino]octanoic acid (18): oil; $[\alpha]_D$ −105.5 (c 0.48, CHCl$_3$); ^{1}H NMR (500 MHz) δ 7.70 (1H, s), 7.39 (1H, d, $J = 10.7$ Hz), 6.92 (1H, d, $J = 10.7$ Hz), 6.85 (1H, br s, NH), 6.53 (1H, s), 4.70 (1H, m), 4.00 (3H, s), 3.95 (3H, s), 3.91 (3H, s), 3.65 (3H, s), 2.52 (1H, br dd, $J \approx 13.5$, 6.2 Hz), 2.40−2.20 (6H, m), 1.86 (1H, m), 1.70−1.55 (4H, m), 1.35−1.25 (4H, br m) (carboxyl proton signal not detected); ^{13}C NMR (125 MHz) δ 181.5*, 179.4, 173.5, 163.7, 153.5, 153.3, 151.1, 141.6, 137.4, 134.4, 125.6 (C), 135.3, 130.9, 113.1, 107.4, 52.3 (CH), 36.7*, 36.2, 35.8, 29.9, 28.9, 28.8, 25.5 (×2) (CH$_2$), 61.6, 61.3, 56.4, 56.1 (CH$_3$) (asterisked signals are low and broad); IR ν_{max} 3300−2600 br (OH, NH), 1714 br, 1652 (C=O) cm^{-1}; HR ESMS m/z 514.2439 (M + H$^+$), calcd for C$_{28}$H$_{36}$NO$_8$, 514.2441.

Data for 12-oxo-12-[(7S)-(1,2,3,10-tetramethoxy-9-oxo-5,6,7,9-tetrahydrobenzo[a]heptalen-7-yl)amino]dodecanoic acid (19): oil; $[\alpha]_D$ −93.6 (c 0.7, CHCl$_3$); ^{1}H NMR (500 MHz) δ 7.74 (1H, s), 7.36 (1H, d, $J = 10.7$ Hz), 6.89 (1H, d, $J = 10.7$ Hz), 6.87 (1H, br s, NH), 6.54 (1H, s), 4.72 (1H, m), 3.99 (3H, s), 3.95 (3H, s), 3.90 (3H, s), 3.65 (3H, s), 2.51 (1H, br dd, $J \approx 13.6$, 6.3 Hz), 2.40−2.20 (6H, br m), 1.83 (1H, m), 1.65−1.55 (4H, br m), 1.35−1.20 (12H, br m) (carboxyl proton signal not detected); ^{13}C NMR (125 MHz) δ 179.6, 177.5*, 173.2, 163.9, 153.5, 152.3, 151.2, 141.7, 137.0, 134.2, 125.6 (C), 135.3, 130.8, 113.0, 107.5, 52.0 (CH), 37.1, 36.2, 34.0*, 29.9, 29.1, 28.9, 28.7−28.5 (four partially overlapped signals), 25.2, 24.7 (CH$_2$), 61.6, 61.3, 56.3, 56.1 (CH$_3$) (asterisked signals are low and broad); IR ν_{max} 3300−2600 br (OH, NH), 1729 br, 1652 (C=O) cm^{-1}; HR ESMS m/z 570.3063 (M + H$^+$), calcd for C$_{32}$H$_{43}$NO$_8$, 570.3067.

Data for 16-oxo-16-[(7S)-(1,2,3,10-tetramethoxy-9-oxo-5,6,7,9-tetrahydrobenzo[a]heptalen-7-yl)amino]hexadecanoic acid (20): oil; $[\alpha]_D$ −68.4 (c 0.12, CHCl$_3$); ^{1}H NMR (500 MHz) δ 7.66 (1H, s), 7.35 (1H, d, $J = 10.7$ Hz), 6.90 (1H, br s, NH), 6.87 (1H, d, $J = 10.7$ Hz), 6.53 (1H, s), 4.71 (1H, m), 3.99 (3H, s), 3.94 (3H, s), 3.90 (3H, s), 3.63 (3H, s), 2.50 (1H, br dd, $J \approx 13.3$, 6.1 Hz), 2.37 (1H, br td, $J \approx 13.3$, 6.7 Hz), 2.35−2.20 (5H, br m), 1.83 (1H, m), 1.65−1.50 (4H, br m), 1.35−1.20 (20H, br m) (carboxyl proton signal not detected); ^{13}C NMR (125 MHz) δ 179.6, 177.5*, 173.1, 164.0, 153.5, 152.2, 151.2, 141.7, 136.9, 134.2, 125.6 (C), 135.4, 130.8, 112.9, 107.5, 52.0 (CH), 37.1, 36.3, 34.0*, 29.9, 29.3−28.8 (10 partially overlapped signals), 25.4, 24.8 (CH$_2$), 61.6, 61.4, 56.4, 56.1 (CH$_3$) (asterisked signals are low and broad); IR ν_{max} 3300 br (OH, NH), 1717 br, 1653 (C=O) cm^{-1}; HR ESMS m/z 626.3696 (M + H$^+$), calcd for C$_{36}$H$_{52}$NO$_8$, 626.3696.

Data for (3R,5S)-5-[(tert-butyldimethylsilyl)oxy]-3-methoxy-6-[(2S)-6-oxo-3,6-dihydro-2H-pyran-2-yl]hexyl 5-oxo-5-{(7S)-(1,2,3,10-tetramethoxy-9-oxo-5,6,7,9-tetrahydrobenzo[a]heptalen-7-yl)amino}pentanoate (23): oil; $[\alpha]_D$ −75.1 (c 0.25, CHCl$_3$); ^{1}H NMR (500 MHz) δ 7.44 (1H, s), 7.25 (1H, d, $J = 10.8$ Hz), 7.10 (1H, br s, NH), 6.82 (1H, br dt, $J = 9.8$, 4.5 Hz), 6.80 (1H, d, $J = 10.8$ Hz), 6.48 (1H, s), 5.96 (1H, br d, $J \approx 9.8$ Hz), 4.61 (1H, m), 4.55 (1H, m), 4.10−4.00 (3H, br m), 3.95 (3H, s), 3.90 (3H, s), 3.86 (3H, s), 3.61 (3H, s), 3.33 (1H, m), 3.27 (3H, s), 2.46 (1H, br dd, $J \approx 13.7$, 6.3 Hz), 2.40−2.15 (8H, br m), 2.00−1.50 (9H, br m), 0.85 (9H, s), 0.05 (3H, s), 0.03 (3H, s); ^{13}C NMR (125 MHz) δ 179.4, 173.0, 171.7, 164.2, 163.9, 153.4, 151.9, 151.1, 141.6, 136.6, 134.2, 125.6, 17.9 (C), 145.3, 135.1, 130.8, 121.3, 112.5, 107.3, 74.7, 74.5, 65.8, 52.1 (CH), 60.9, 43.1, 42.9, 36.7, 34.9, 33.4, 32.6, 29.9, 29.8, 20.6 (CH$_2$), 61.5, 61.3, 56.3, 56.1, 56.0, 25.8 (×3), −4.4, −4.6 (CH$_3$); IR ν_{max} 3300 br (NH), 1731 br, 1674 (C=O) cm^{-1}; HR ESMS m/z 812.4041 (M + H$^+$), calcd for C$_{43}$H$_{62}$NO$_{12}$Si, 812.4050.

Data for (3R,5S)-5-[(tert-butyldimethylsilyl)oxy]-3-methoxy-6-[(2S)-6-oxo-3,6-dihydro-2H-pyran-2-yl]hexyl 8-oxo-8-{(7S)-(1,2,3,10-tetramethoxy-9-oxo-5,6,7,9-tetrahydrobenzo[a]heptalen-7-yl)amino}octanoate (24): oil; $[\alpha]_D$ −87.2 (c 0.74, CHCl$_3$); ^{1}H NMR (500 MHz) δ 7.39 (1H, s), 7.28 (1H, d, $J = 10.8$ Hz), 6.89 (1H, dt, $J = 9.8$, 4 Hz), 6.80 (1H, d, $J = 10.8$ Hz), 6.53 (1H,

s), 6.50 (1H, br d, $J \approx$ 7 Hz, NH), 6.02 (1H, br d, $J \approx$ 9.8 Hz), 4.70−4.55 (2H, m), 4.20−4.05 (3H, br m), 3.98 (3H, s), 3.94 (3H, s), 3.90 (3H, s), 3.65 (3H, s), 3.40 (1H, m), 3.31 (3H, s), 2.52 (1H, br dd, $J \approx$ 13.7, 6.3 Hz), 2.41 (1H, br td, $J \approx$ 13.2, 6.8 Hz), 2.35−2.20 (5H, br m), 2.00 (1H, m), 1.90−1.50 (12H, br m), 1.35−1.20 (4H, br m), 0.88 (9H, s), 0.07 (3H, s), 0.05 (3H, s); ^{13}C NMR (125 MHz) δ 179.4, 173.6, 172.5, 164.3, 164.0, 153.4, 151.3, 151.1, 141.8, 136.3, 134.1, 125.7, 18.0 (C), 145.3, 135.1, 130.8, 121.5, 112.2, 107.4, 74.9, 74.6, 65.9, 52.0 (CH), 60.8, 43.3, 43.2, 37.0, 36.3, 34.2, 32.7, 30.0, 29.9, 28.8, 28.7, 25.2, 24.7 (CH$_2$), 61.6, 61.4, 56.3, 56.2, 56.1, 25.9 (×3), −4.3, −4.6 (CH$_3$); IR ν_{max} 3300 br (NH), 1731 br, 1674 (C=O) cm^{-1}; HR ESMS m/z 854.4509 (M + H$^+$), calcd for C$_{46}$H$_{68}$NO$_{12}$Si, 854.4511.

Data for (3R,5S)-5-[(tert-butyldimethylsilyl)oxy]-3-methoxy-6-[(2S)-6-oxo-3,6-dihydro-2H-pyran-2-yl]hexyl 12-oxo-12-{(7S)-(1,2,3,10-tetramethoxy-9-oxo-5,6,7,9-tetrahydrobenzo-[a]heptalen-7-yl)amino}dodecanoate (25): oil; [α]$_D$ −72.8 (c 1.1, CHCl$_3$); ^{1}H NMR (500 MHz) δ 7.44 (1H, s, H-8), 7.29 (1H, d, J = 10.7 Hz, H-12), 6.90 (1H, br d, $J \approx$ 7.5 Hz, NH), 6.88 (1H, overlapped m, H-3′), 6.82 (1H, d, J = 10.7 Hz, H-11), 6.52 (1H, s, H-4), 6.00 (1H, dt, J = 9.8, 1.5 Hz, H-2′), 4.65 (1H, m, H-7), 4.57 (1H, m, H-5′), 4.15−4.05 (3H, br m, H-7′, H-11′), 3.98 (3H, s, OMe), 3.94 (3H, s, OMe), 3.89 (3H, s, OMe), 3.65 (3H, s, OMe), 3.40 (1H, m, H-9′), 3.30 (3H, s, 9′-OMe), 2.50 (1H, br dd, $J \approx$ 13.3, 6 Hz, H-5α or H-5β), 2.38 (1H, br td, $J \approx$ 13.2, 6.8 Hz, H-5β or H-5α), 2.35−2.15 (7H, br m, H-6α or H-6β, H-4′, H-13′, H-22′), 2.00 (1H, ddd, J = 14, 9.3, 3.5 Hz, H-6β or H-6α), 1.80−1.50 (10H, br m, H-6′, H-8′, H-10′, H-14′, H-21′), 1.35−1.20 (12H, br m, H-15′ to H-20′), 0.86 (9H, s, tBuSi), 0.07 (3H, s, MeSi), 0.05 (3H, s, MeSi); ^{13}C NMR (125 MHz) δ 179.4 (C-9), 173.6 (C-12′), 172.7 (C-23′), 164.1 (C-1′), 163.9 (C-10), 153.4 (C-3), 151.8 (C-7a), 151.1 (C-1), 145.1 (C-3′), 141.6 (C-2), 136.4 (C-12a), 135.1 (C-12), 134.1 (C-4a), 130.6 (C-8), 125.7 (C-12b), 121.4 (C-2′), 112.4 (C-11), 107.3 (C-4), 74.8 (C-9′), 74.4 (C-5′), 65.9 (C-7′), 60.7 (C-11′), 61.5, 61.3, 56.3, 56.1 (×2) (five OMe groups), 52.0 (C-7), 43.3, 43.1 (C-6′, H-8′), 34.2 (C-10′), 36.7, 36.1, 32.6 (C-6, C-13′, C-22′), 29.9 (C-5), 29.3−29.0 (seven partially overlapped signals), 25.3, 24.8 (all remaining methylene groups), 25.8 (×3) (Me$_3$CSi), 17.9 (Me$_3$CSi), −4.4, −4.5 (SiMe$_2$); IR ν_{max} 3300 br (NH), 1732 br, 1674 (C=O) cm^{-1}; HR ESMS m/z 910.5111 (M + H$^+$), calcd for C$_{50}$H$_{76}$NO$_{12}$Si, 910.5117. NMR signals of this compound were assigned with the aid of 2D homo- and heteronuclear pulse sequences (COSY, HSQC, HMBC). For atom numbering see the Supporting Information. Signal assignments within the colchicine fragment were consistent with literature data for colchicine.[33]

Data for (3R,5S)-5-[(tert-butyldimethylsilyl)oxy]-3-methoxy-6-[(2S)-6-oxo-3,6-dihydro-2H-pyran-2-yl]hexyl 16-oxo-16-{(7S)-(1,2,3,10-tetramethoxy-9-oxo-5,6,7,9-tetrahydrobenzo-[a]heptalen-7-yl)amino}hexadecanoate (26): oil; [α]$_D$ −73.4 (c 0.84, CHCl$_3$); ^{1}H NMR (500 MHz) δ 7.42 (1H, s), 7.29 (1H, d, J = 10.7 Hz), 6.88 (1H, dt, J = 9.8, 4.5 Hz), 6.82 (1H, d, J = 10.7 Hz), 6.78 (1H, br d, $J \approx$ 7 Hz, NH), 6.51 (1H, s), 6.01 (1H, dt, J = 9.8, 1.5 Hz), 4.65 (1H, m), 4.58 (1H, m), 4.20−4.05 (3H, br m), 3.98 (3H, s), 3.94 (3H, s), 3.89 (3H, s), 3.65 (3H, s), 3.40 (1H, m), 3.30 (3H, s), 2.50 (1H, br dd, $J \approx$ 13.3, 6 Hz), 2.39 (1H, br td, $J \approx$ 13.2, 6.8 Hz), 2.35−2.15 (7H, br m), 2.00 (1H, ddd, J = 14, 9.3, 3.5 Hz), 1.85−1.50 (10H, br m), 1.35−1.20 (20H, br m), 0.87 (9H, s), 0.09 (3H, s), 0.06 (3H, s); ^{13}C NMR (125 MHz) δ 179.4, 173.8, 172.7, 164.2, 164.0, 153.4, 151.5, 151.3, 141.7, 136.4, 134.2, 125.7, 18.0 (C), 145.1, 135.1, 130.7, 121.5, 112.3, 107.4, 74.9, 74.5, 65.9, 52.0 (CH), 60.8, 43.4, 43.2, 36.9, 36.4, 34.3, 32.7, 30.0, 29.9, 29.6−29.2 (10 partially overlapped signals), 25.4, 25.0 (CH$_2$), 61.6, 61.4, 56.3, 56.2, 56.1, 25.9 (×3), −4.3, −4.4 (CH$_3$); IR ν_{max} 3300 br (NH), 1733 br, 1675 (C=O) cm^{-1}; HR ESMS m/z 966.5756 (M + H$^+$), calcd for C$_{54}$H$_{84}$NO$_{12}$Si, 966.5763.

Biological Methods. Cell Culture. Cell culture media were purchased from Gibco (Grand Island, NY). Fetal bovine serum (FBS) was a product of Harlan-Seralab (Belton, U.K.). Supplements and other chemicals not listed in this section were obtained from Sigma Chemical Co. (St. Louis, MO). Plastics for cell culture were supplied by Thermo Scientific BioLite. All tested compounds were dissolved in DMSO at a concentration of 10 μg/mL and stored at −20 °C until use.

HT-29, MCF-7, and HEK-293 cell lines were maintained in Dulbecco's modified Eagle's medium (DMEM) containing glucose (1 g/L), glutamine (2 mM), penicillin (50 IU/mL), streptomycin (50 μg/mL), and amphoterycin (1.25 μg/mL), supplemented with 10% FBS.

Human A-549 non-small-cell lung carcinoma cells were cultured in RPMI 1640 supplemented with 10% fetal calf serum (FCS), glutamine, and antibiotics as previously described.[30] Human ovarian carcinomas A2780 and A2780AD (MDR (multidrug resistance) overexpressing P-glycoprotein) cell lines were cultured as above with the addition of 0.25 unit/mL bovine insulin.

Cytotoxicity Assays, Indirect Immunofluorescence, and Cell Cycle. The 3-(4,5-dimethylthiazol-2-yl)-2,5-diphenyltetrazolium bromide (MTT; Sigma Chemical Co.) dye reduction assay in 96-well microplates was used, as previously described.[34] A total of 5 × 10^3 HT-29, MCF-7, or HEK-293 cells in a total volume of 100 μL of their respective growth media were incubated with serial dilutions of the tested compounds. After 3 days of incubation (37 °C, 5% CO$_2$ in a humid atmosphere), 10 μL of MTT (5 mg/mL in phophate-buffered saline (PBS)) was added to each well, and the plate was incubated for a further 4 h (37 °C). The resulting formazan was dissolved in 150 μL of 0.04 N HCl/2-propanol and read at 550 nm. All determinations were carried out in triplicate.

Cytotoxic evaluation on A2780 and A2780AD cells was performed with the MTT assay modified as previously described.[35] Indirect immunofluorescence was performed in A549 cells that had been cultured overnight in 12 mm round coverslips and incubated for a further 24 h in the absence (drug vehicle DMSO) or in the presence of different ligand concentrations. Attached cells were permeabilized with Triton X100 and fixed with 3.7% formaldehyde. Microtubules were specifically stained with DM1A α-tubulin monoclonal antibodies, and DNA was stained with Hoechst 33342 as previously described.[36] The preparations were examined using a Zeiss axioplan epifluorescence microscope, and the images were recorded with a Hamamatsu 4742-95 cooled charge-coupled device (CCD) camera. Progression through the cell cycle analysis was assessed by flow cytometry DNA determination with propidium iodide. Cells were fixed, treated with RNase, and stained with propidium iodide as previously described.[37] Analysis was performed with a Coulter Epics XL flow cytometer.

Tubulin Assembly Inhibition Assay. The effect of the compounds on the assembly of purified tubulin (Table 3) was determined by incubating 20 μM purified tubulin at 37 °C for 30 min in GAB (3.4 M glycerol, 10 mM sodium phosphate, 1 mM EGTA, 1 mM GTP, pH 6.5) in the presence of 25 μM pironetin, colchicine, and docetaxel (a microtubule-stabilizing ligand as a positive control) and a 30 μM concentration each of compounds **1**, **3**, **9**, and **11** or 2 μL of DMSO (vehicle). The samples were processed, and the critical concentration for tubulin assembly[29] in the presence of the ligands was calculated as described.[38] The results of Table 4 were obtained with the same methodology except for the changes in ligand concentrations. The numerical data mentioned in the tables represent average values of five measurements. Errors are standard errors of the average.

Interaction of Compounds with Tubulin at Equimolecular Concentration. A 30 μM final solution each of compounds **1**, **3**, **9**, and **11** (previously dissolved at 10 mM in dimethyl sulfoxide) in a buffer mixture (10 mM sodium phosphate, 30% glycerol, 1 mM EGTA, 1 mM GTP, 6 mM MgCl$_2$) was mixed with a 30 μM final solution of tubulin in the same buffer. The mixture was allowed to stand for 1 h at 37 °C and extracted with dichloromethane. This yielded solution A, which was analyzed for its content in the respective ligand.

A 30 μM final solution each of compounds **1**, **3**, **9**, and **11** (previously dissolved at 10 mM in dimethyl sulfoxide) in a buffer mixture (10 mM sodium phosphate, 30% glycerol, 1 mM EGTA, 1 mM GTP, 6 mM MgCl$_2$) was mixed with a 30 μM final solution of tubulin in the same buffer. The mixture was allowed to stand for 1 h at 37 °C to allow for the formation of microtubules and then ultracentrifuged. The supernatant solution and the solid pellet were then separated and extracted with dichloromethane. This yielded

solutions B and C, respectively, which were analyzed for their content in the respective ligand.

ASSOCIATED CONTENT

Supporting Information

Structures of the synthetic targets and intermediates and NMR spectra of all new compounds. This material is available free of charge via the Internet at http://pubs.acs.org.

AUTHOR INFORMATION

Corresponding Authors
*E-mail: fer@cib.csic.es (for the biochemical part).
*E-mail: i.barasoain@cib.csic.es (for the biological part).
*E-mail: alberto.marco@uv.es (for the chemical part).

Notes
The authors declare no competing financial interest.

ACKNOWLEDGMENTS

ABBREVIATIONS USED

TBMs, tubulin-binding molecules; NMM, N-methylmorpholine; HT-29, human colon adenocarcinoma cells; MCF-7, breast adenocarcinoma cells; HEK-293, human embryonic kidney cells; A2780, ovarian carcinoma cells sensitive to chemotherapy; A2780AD, ovarian carcinoma cells resistant to chemotherapy

REFERENCES

(1) Garcia, M.; Jemal, A.; Ward, E. M.; Center, M. M.; Hao, Y.; Siegel, R. L.; Thun, M. J. *Global Cancer Facts & Figures 2007*; American Cancer Society: Atlanta, GA, 2007.

(2) (a) Hanahan, D.; Weinberg, R. A. The hallmarks of cancer. *Cell* **2000**, *100*, 57−70. (b) Stratton, M. R.; Campbell, P. J.; Futreal, P. A. The cancer genome. *Nature* **2009**, *458*, 719−724. (c) Hanahan, D.; Weinberg, R. A. The hallmarks of cancer: the next generation. *Cell* **2011**, *144*, 646−674.

(3) (a) Boyle, F. T.; Costello, G. F. Cancer therapy: a move to the molecular level. *Chem. Soc. Rev.* **1998**, *27*, 251−261. (b) Gibbs, J. B. Mechanism-based target identification and drug discovery in cancer research. *Science* **2000**, *287*, 1969−1973.

(4) (a) Penn, L. Z. Apoptosis modulators as cancer therapeutics. *Curr. Opin. Invest. Drugs* **2001**, *2*, 684−692. (b) Zhou, B.; Liu, Z.-L. Bioantioxidants: from chemistry to biology. *Pure Appl. Chem.* **2005**, *77*, 1887−1903. (c) Park, H.-J.; Jung, H.-J.; Lee, K.-T.; Choi, J. Biological characterization of the chemical structures of naturally occurring substances with cytotoxicity. *Nat. Prod. Sci.* **2006**, *12*, 175−192.

(d) Portt, L.; Norman, G.; Clapp, C.; Greenwood, M.; Greenwood, M. T. Anti-apoptosis and cell survival: a review. *Biochim. Biophys. Acta, Mol. Cell Res.* **2011**, *1813*, 238−259. (e) Torres-Andón, F.; Fadeel, B. Programmed cell death: molecular mechanisms and implications for safety assessment of nanomaterials. *Acc. Chem. Res.* **2013**, *46*, 733−742.

(5) (a) Sánchez-Pedregal, V. M.; Griesinger, C. The tubulin binding mode of MT stabilizing and destabilizing agents studied by NMR. *Top. Curr. Chem.* **2009**, *286*, 151−208. (b) Nettles, J. H.; Downing, K. H. The tubulin binding mode of microtubule stabilizing agents studied by electron crystallography. *Top. Curr. Chem.* **2009**, *286*, 209−257. (c) Botta, M.; Forli, S.; Magnani, M.; Manetti, F. Molecular modeling approaches to study the binding mode on tubulin of microtubule destabilizing and stabilizing agents. *Top. Curr. Chem.* **2009**, *286*, 279−328. (d) Alushin, G. M.; Lander, G. C.; Kellogg, E. H.; Zhang, R.; Baker, D.; Nogales, E. High-resolution microtubule structures reveal the structural transitions in αβ-tubulin upon GTP hydrolysis. *Cell* **2014**, *157*, 1117−1129.

(6) Chen, J.; Liu, T.; Dong, X.; Hu, Y. Recent development and SAR analysis of colchicine binding site inhibitors. *Mini-Rev. Med. Chem.* **2009**, *9*, 1174−1190.

(7) (a) Van der Heijden, R.; Jacobs, D. I.; Snoeijer, W.; Hallard, D.; Verpoorte, R. The *Catharanthus* alkaloids: pharmacognosy and biotechnology. *Curr. Med. Chem.* **2004**, *11*, 607−628. (b) Keglevich, P.; Hazai, L.; Kalaus, G.; Szántay, C. Modifications on the basic skeletons of vinblastine and vincristine. *Molecules* **2012**, *17*, 5893−5914.

(8) Fu, Y.; Li, S.; Zu, Y.; Yang, G.; Yang, Z.; Luo, M.; Jiang, S.; Wink, M.; Efferth, T. Medicinal chemistry of paclitaxel and its analogs. *Curr. Med. Chem.* **2009**, *16*, 3966−3985.

(9) (a) Jordan, M. A. Mechanism of action of antitumor drugs that interact with microtubules and tubulin. *Curr. Med. Chem.: Anti-Cancer Agents* **2002**, *2*, 1−17. (b) Abal, M.; Andreu, J. M.; Barasoain, I. Taxanes: microtubule and centrosome targets, and cell cycle dependent mechanisms of action. *Curr. Cancer Drug Targets* **2003**, *3*, 193−203.

(10) (a) Correia, J. J.; Lobert, S. Physiochemical aspects of tubulin-interacting antimitotic drugs. *Curr. Pharm. Des.* **2001**, *7*, 1213−1228. (b) Jiménez-Barbero, J.; Amat-Guerri, F.; Snyder, J. P. The solid state, solution and tubulin-bound conformations of agents that promote microtubule stabilization. *Curr. Med. Chem.: Anti-Cancer Agents* **2002**, *2*, 91−122. (c) Díaz, J. F.; Andreu, J. M.; Jiménez-Barbero, J. The interaction of microtubule with stabilizers characterized at biochemical and structural levels. *Top. Curr. Chem.* **2009**, *286*, 121−149. (d) Gigant, B.; Cormier, A.; Dorléans, A.; Ravelli, R. B. G.; Knossow, M. Microtubule-destabilizing agents: structural and mechanistic insights from the interaction of colchicine and vinblastine with tubulin. *Top. Curr. Chem.* **2009**, *286*, 259−278. (e) Daly, E. M.; Taylor, R. E. Entropy and enthalpy in the activity of tubulin-based antimitotic agents. *Curr. Chem. Biol.* **2009**, *3*, 367−379.

(11) Sarabia, F.; García-Castro, M.; Sánchez-Ruiz, A. Chemistry and biology of novel microtubule-destabilizing agents that bind α-tubulin. *Curr. Bioact. Compd.* **2006**, *2*, 269−299.

(12) Anderson, H. J.; Coleman, J. E.; Andersen, R. J.; Roberge, M. Cytotoxic peptides hemiasterlin, hemiasterlin A, and hemiasterlin B include mitotic arrest and abnormal spindle formation. *Cancer Chemother. Pharmacol.* **1997**, *39*, 223−226.

(13) (a) Kondoh, M.; Usui, T.; Kobayashi, S.; Tsuchiya, K.; Nishikawa, K.; Nishikiori, T.; Mayumi, T.; Osada, H. Cell cycle arrest and antitumor activity of pironetin and its derivatives. *Cancer Lett.* **1998**, *126*, 29−32. (b) Kondoh, M.; Usui, T.; Nishikiori, T.; Mayumi, T.; Osada, H. Apoptosis induction via microtubule disassembly by an antitumour compound, pironetin. *Biochem. J.* **1999**, *340*, 411−416. (c) Watanabe, H.; Watanabe, H.; Usui, T.; Kondoh, M.; Osada, H.; Kitahara, T. Synthesis of pironetin and related analogs: studies on structure-activity relationships as tubulin assembly inhibitors. *J. Antibiot.* **2000**, *53*, 540−545. (d) Usui, T.; Watanabe, H.; Nakayama, H.; Tada, Y.; Kanoh, N.; Kondoh, M.; Asao, T.; Takio, K.; Watanabe, H.; Nishikawa, K.; Kitahara, T.; Osada, H. The

anticancer natural product pironetin selectively targets Lys352 of α-tubulin. *Chem. Biol.* **2004**, *11*, 799−806.

(14) For two recent reviews on the chemical and pharmacological aspects of 5,6-dihydropyran-2-ones, see: (a) Marco, J. A.; Carda, M.; Murga, J.; Falomir, E. Stereoselective syntheses of naturally occurring 5,6-dihydropyran-2-ones. *Tetrahedron* **2007**, *63*, 2929−2958. (b) Marco, J. A.; Carda, M. Recent advances in the field of naturally occurring 5,6-dihydropyran-2-ones. In *Natural Lactones and Lactams. Synthesis, Occurrence and Biological Activity*; Janecki, T., Ed.; Wiley-VCH: Weinheim, Germany, 2014; pp 51−100.

(15) (a) Kavallaris, M. Microtubules and resistance to tubulin-binding agents. *Nat. Rev. Cancer* **2010**, *10*, 194−204. (b) Holohan, C.; Van Schaeybroeck, S.; Longley, D. B.; Johnston, P. G. Cancer drug resistance: an evolving paradigm. *Nat. Rev. Cancer* **2013**, *13*, 714−726.

(16) (a) Rossi, L. M.; Rangasamy, P.; Zhang, J.; Qiu, X.-Q.; Wu, G. Y. Research advances in the development of peptide antibiotics. *J. Pharm. Sci.* **2007**, *97*, 1060−1070. (b) Courvalin, P. Predictable and unpredictable evolution of antibiotic resistance. *J. Intern. Med.* **2008**, *264*, 4−16. (c) Gualtieri, M.; Baneres-Roquet, F.; Villain-Guillot, P.; Pugniere, M.; Leonetti, J.-P. The antibiotics in the chemical space. *Curr. Med. Chem.* **2009**, *16*, 390−393.

(17) (a) Yasui, K.; Tamura, Y.; Nakatani, K.; Kawada, K.; Ohtani, M. Total synthesis of (−)-PA-48153C, a novel immunosuppressive 2-pyranone derivative. *J. Org. Chem.* **1995**, *60*, 7567−7574. (b) Gurjar, M. K.; Henri, J. T., Jr.; Bose, D. S.; Rao, A. V. R. Total synthesis of a potent immunosuppressant pironetin. *Tetrahedron Lett.* **1996**, *37*, 6615−6618. (c) Chida, N.; Yoshinaga, M.; Tobe, T.; Ogawa, S. Total synthesis of (−)-PA-48153C (pironetin) utilising l-quebrachitol as a chiral building block. *Chem. Commun.* **1997**, 1043−1044. (d) Watanabe, H.; Watanabe, H.; Bando, M.; Kido, M.; Kitahara, T. An efficient synthesis of pironetins employing a useful chiral building block, (1S,5S,6R)-5-hydroxybicyclo[4.1.0]heptan-2-one. *Tetrahedron* **1999**, *55*, 9755−9776. (e) Keck, G. E.; Knutson, C. E.; Wiles, S. A. Total synthesis of the immunosupressant (−)-pironetin (PA48153C). *Org. Lett.* **2001**, *3*, 707−710. (f) Dias, L. C.; de Oliveira, L. G.; de Sousa, M. A. Total synthesis of (−)-pironetin. *Org. Lett.* **2003**, *5*, 265−268. (g) Shen, X.; Wasmuth, A. S.; Zhao, J.; Zhu, C.; Nelson, S. G. Catalytic asymmetric assembly of stereodefined propionate units: an enantioselective total synthesis of (−)-pironetin. *J. Am. Chem. Soc.* **2006**, *128*, 7438−7439. (h) Enders, D.; Dhulut, S.; Steinbusch, D.; Herrbach, A. Asymmetric total synthesis of (−)-pironetin employing the SAMP/RAMP hydrazone methodology. *Chem.—Eur. J.* **2007**, *13*, 3942−3949. (i) Bressy, C.; Vors, J.-P.; Hillebrand, S.; Arseniyadis, S.; Cossy, J. Asymmetric total synthesis of the immunosuppressant (−)-pironetin. *Angew. Chem., Int. Ed.* **2008**, *47*, 10137−10140. (j) Crimmins, M. T.; Dechert, A.-M. R. Enantioselective total synthesis of (−)-pironetin: iterative aldol reactions of thiazolidinethiones. *Org. Lett.* **2009**, *11*, 1635−1638. (k) Yadav, J. S.; Ather, H.; Rao, N. V.; Reddy, M. S.; Prasad, A. R. Stereoselective synthesis of (−)-pironetin by an iterative Prins cyclisation and reductive cleavage strategy. *Synlett* **2010**, 1205−1208.

(18) See our previous papers in this area: (a) Marco, J. A.; García-Pla, J.; Carda, M.; Murga, J.; Falomir, E.; Trigili, C.; Notararigo, S.; Díaz, J. F.; Barasoain, I. Design and synthesis of pironetin analogues with simplified structure and study of their interactions with microtubules. *Eur. J. Med. Chem.* **2011**, *46*, 1630−1637. (b) Carda, M.; Murga, J.; Díaz-Oltra, S.; García-Pla, J.; Paños, J.; Falomir, E.; Trigili, C.; Díaz, J. F.; Barasoain, I.; Marco, J. A. Synthesis and biological evaluation of α-tubulin-binding pironetin analogues with enhanced lipophilicity. *Eur. J. Org. Chem.* **2013**, 1116−1123. (c) Paños, J.; Díaz-Oltra, S.; Sánchez-Peris, M.; García-Pla, J.; Murga, J.; Falomir, E.; Carda, M.; Redondo-Horcajo, M.; Díaz, J. F.; Barasoain, I.; Marco, J. A. Synthesis and biological evaluation of truncated α-tubulin-binding pironetin analogues lacking alkyl pendants in the side chain or the dihydropyrone ring. *Org. Biomol. Chem.* **2013**, *11*, 5809−5826.

(19) Vilanova, C. Ph.D. Thesis, Universitat Jaume I, December 2013.

(20) For some selected reviews on the interest and utility of hybrid molecules in medicine and pharmacology, see: (a) Hanessian, S. Structure-based organic synthesis of drug prototypes: a personal odyssey. *ChemMedChem* **2006**, *1*, 1300−1330. (b) Meunier, B. Hybrid molecules with a dual mode of action: dream or reality? *Acc. Chem. Res.* **2008**, *41*, 69−77. (c) Decker, M. Hybrid molecules incorporating natural products: applications in cancer therapy, neurodegenerative disorders and beyond. *Curr. Med. Chem.* **2011**, *18*, 1464−1475.

(21) For hybrid molecules containing colchicine fragments, see, for example: (a) Bombuwala, K.; Kinstle, T.; Popik, V.; Uppal, S. O.; Olesen, J. B.; Viña, J.; Heckman, C. A. Colchitaxel, a coupled compound made from microtubule inhibitors colchicine and paclitaxel. *Beilstein J. Org. Chem.* **2006**, *2*, No. 13. (b) Sharifi, N.; Hamel, E.; Lill, M. A.; Risbood, P.; Kane, C. T., Jr.; Hossain, M. T.; Jones, A.; Dalton, J. T.; Farrar, W. L. A bifunctional colchicinoid that binds to the androgen receptor. *Mol. Cancer Ther.* **2007**, *6*, 2328−2336. (c) Zefirova, O. N.; Nurieva, E. V.; Shishov, D. V.; Bashkin, I. I.; Fuchs, F.; Lemcke, H.; Schröder, F.; Weiss, D. G.; Zefirov, N. S.; Kuznetsov, S. A. Synthesis and SAR requirements of adamantane−colchicine conjugates with both microtubule depolymerizing and tubulin clustering activities. *Bioorg. Med. Chem.* **2011**, *19*, 5529−5538. (d) Malysheva, Y. B.; Combes, S.; Allegro, D.; Peyrot, V.; Knochel, P.; Gavryushin, A. E.; Fedorov, A. Y. Synthesis and biological evaluation of novel anticancer bivalent colchicine−tubulizine hybrids. *Bioorg. Med. Chem.* **2012**, *20*, 4271−4278. (e) Zhang, X.; Zhang, J.; Tong, L.; Luo, Y.; Su, M.; Zang, Y.; Li, J.; Lu, W.; Chen, Y. The discovery of colchicine-SAHA hybrids as a new class of antitumor agents. *Bioorg. Med. Chem.* **2013**, *21*, 3240−3244.

(22) Even though the distance between the pironetin and colchicine binding sites is not yet known with complete accuracy, an examination of the available X-ray data of tubulin[10d] reveals that the aliphatic carbon chains of compounds **1**−**12** are not sufficiently long as to permit a simultaneous binding to both sites. However, we have not tried to prepare derivatives with still longer chains because this would give highly hydrophobic compounds with a too low solubility in polar media.

(23) Bagnato, J. D.; Eilers, A. L.; Horton, R. A.; Grissom, C. B. Synthesis and characterization of a cobalamin-colchicine conjugate as a novel tumor-targeted cytotoxin. *J. Org. Chem.* **2004**, *69*, 8987−8996.

(24) Torijano-Gutiérrez, S.; Vilanova, C.; Díaz-Oltra, S.; Murga, J.; Falomir, E.; Carda, M.; Marco, J. A. Design and synthesis of pironetin analogue/combretastatin A-4 hybrids and evaluation of their cytotoxic activity. *Eur. J. Org. Chem.* **2014**, 2284−2296.

(25) Inanaga, J.; Hirata, K.; Saeki, H.; Katsuki, T.; Yamaguchi, M. A rapid esterification by mixed anhydride and its application to large-ring lactonization. *Bull. Chem. Soc. Jpn.* **1979**, *52*, 1989−1993.

(26) Arden, N.; Betenbaugh, M. J. Life and death in mammalian cell culture: strategies for apoptosis inhibition. *Trends Biotechnol.* **2004**, *22*, 174−180.

(27) Gadgeel, S. M. New targets in non-small cell lung cancer. *Curr. Oncol. Rep.* **2013**, *15*, 411−423.

(28) Jordan, M. A.; Thrower, D.; Wilson, L. Effects of vinblastine, podophyllotoxin and nocodazole on mitotic spindles. Implications for the role of microtubule dynamics in mitosis. *J. Cell Sci.* **1992**, *102*, 401−416.

(29) Oosawa, F.; Asakura, S. *Thermodynamics of the Polymerization of Proteins*; Academic Press: London, 1975.

(30) Buey, R. M.; Calvo, E.; Barasoain, I.; Pineda, O.; Edler, M. C.; Matesanz, R.; Cerezo, G.; Vanderwal, C. D.; Day, B. W.; Sorensen, E. J.; López, J. A.; Andreu, J. M.; Hamel, E.; Díaz, J. F. Cyclostreptin binds covalently to microtubule pores and lumenal taxoid binding sites. *Nat. Chem. Biol.* **2007**, *3*, 117−125.

(31) Ravelli, R. B. G.; Gigant, B.; Curmi, P. A.; Jourdain, I.; Lachkar, S.; Sobel, A.; Knossow, M. Insight into tubulin regulation from a complex with colchicine and a stathmin-like domain. *Nature* **2004**, *428*, 198−202.

(32) (a) Sun, L.; Hamel, E.; Lin, C. M.; Hastie, S. B.; Pyluck, A.; Lee, K. H. Antitumor agents. 141. Synthesis and biological evaluation of novel thiocolchicine analogs: *N*-acyl, *N*-aroyl-, and *N*-(substituted benzyl)-deacetylthiocolchicines as potent cytotoxic and antimitotic compounds. *J. Med. Chem.* **1993**, *36*, 1474−1479. (b) Bhattacharyya, B.; Howard, R.; Maity, S. N.; Brossi, A.; Sharma, P. N.; Wolff, J. B ring

regulation of colchicine binding kinetics and fluorescence. *Proc. Natl. Acad. Sci. U.S.A.* **1986**, *83*, 2052−2055.

(33) Meksuriyen, D.; Lin, L. J.; Cordell, G. A.; Mukhopadhyay, S.; Banerjee, S. K. NMR Studies of colchicine and its photoisomers, *β*- and *γ*-lumicolchicines. *J. Nat. Prod.* **1988**, *51*, 88−93.

(34) Rodríguez-Nieto, S.; Medina, M. A.; Quesada, A. R. A re-evaluation of fumagillin selectivity towards endothelial cells. *Anticancer Res.* **2001**, *21*, 3457−3460.

(35) Yang, C.; Barasoain, I.; Li, X.; Matesanz, R.; Liu, R.; Sharom, F. J.; Yin, D. L.; Díaz, J. F.; Fang, W. S. Overcoming tumor drug resistance mediated by P-glycoprotein overexpression with high affinity taxanes: a SAR study of C-2 modified 7-acyl-10-deacetilcephalomannines. *ChemMedChem* **2007**, *2*, 691−701.

(36) De Ines, C.; Leynadier, D.; Barasoain, I.; Peyrot, V.; Garcia, P.; Briand, C.; Rener, G. A.; Temple, C., Jr. Inhibition of microtubules and cell-cycle arrest by a new 1-deaza-7,8-dihydropteridine antitumor drug, CI-980, and by its chiral isomer, NSC-613863. *Cancer Res.* **1994**, *54*, 75−84.

(37) Andreu, J. M.; Barasoain, I. The interaction of baccatin III with the taxol binding site of microtubules determined by a homogeneous assay with fluorescent taxoid. *Biochemistry* **2001**, *40*, 11975−11984.

(38) Buey, R. M.; Barasoain, I.; Jackson, E.; Meyer, A.; Giannakakou, P.; Paterson, I.; Mooberry, S.; Andreu, J. M.; Díaz, J. F. Microtubule interactions with chemically diverse stabilizing agents: thermodynamics of binding to the paclitaxel site predicts cytotoxicity. *Chem. Biol.* **2005**, *12*, 1269−1279.